

**BIOLOGICAL EFFECTS OF LOW DOSE RADIATION FROM  
COMPUTERIZED TOMOGRAPHY SCANS**

By

ANGELICA ASIS, B.Sc. (Hons)

A thesis

Submitted to the School of Graduate Studies in  
Partial Fulfillment of the Requirements for the Degree  
Master of Science

McMaster University

©Copyright by Angelica Asis, January 2011

MASTER OF SCIENCE (2010)

McMaster University

(Radiation Biology)

Hamilton, Ontario

TITLE:                    Biological Effects of Low Dose Radiation from  
Computerized Tomography Scans

AUTHOR:                Angelica Asis

SUPERVISOR:         Professor D. R. Boreham

NUMBER OF PAGES: x, 84

## Abstract

Humans have evolved under a field of low level radiation, and continue to be exposed to ubiquitous levels from natural and man-made sources including diagnostic radiology. The computerized tomography scan, in particular, plays an important role in the investigation of disease and its use increased dramatically over the years. This raises the concern that elevation in radiation exposure from x-ray modalities may increase an individual's risk for cancer. The purpose of this study is to help address this issue by measuring biological changes in lymphocytes before and after a CT scan. Venous blood was collected from eight prostate cancer patients before and after their scan and delivered to McMaster University at room temperature. For the dicentric assay, 0.5 ml whole blood/tube was irradiated with 3 Gy gamma rays using a Cs<sup>137</sup> source and then incubated at 37°C for 46 hours. Metaphases were scored by microscopy. For apoptosis and  $\gamma$ -H2AX, lymphocytes in media were irradiated on ice with 8 Gy and analyzed by flow cytometry. Biological effects *in vivo* from the CT scan were minimal for all endpoints when averaged between all donors. Overall, there was a high degree of inter-individual variation for each effect, although no correlation was found between dose (dose length product) from CT and apoptosis as well as the induction of  $\gamma$ -H2AX foci. The adaptive response also showed patient variation, and the frequency of dicentrics was the only endpoint that was lower overall following CT + 3Gy in comparison to 3 Gy alone. This research presents a challenge to current linear models of radiation associated genetic risk, and shows that individuals respond to radiation differently depending on biological factors.

## Acknowledgements

I would like to thank my supervisor Dr. Douglas Boreham for providing me with the opportunity to undertake this research, his ongoing support, and tireless patience throughout the duration of my program. I would also like to extend my gratitude to the other members of my committee board, including Dr. Ian Dayes, who assisted me in planning and carrying out this research using samples collected from his patients, and Dr. Gianni Parise for his time and advice.

A huge thank you goes out to our lab technicians who worked seemingly endless hours to help get this work complete. Sincere thanks to Lisa Laframboise, Nicole McFarlane and Mary Ellen Cybulski for their guidance, lab support and insightful suggestions over the past couple of years.

I want to thank my peers, especially Kristina, Nghi, Emma, Alex, Caitlin, and Steve for their ongoing encouragement, friendship, support and advice throughout the course of my program. I honestly could not have made it here without you and I appreciate every experience we've endured together, from long nights in the lab to our crazy adventures at conferences. I am also very grateful for the help from our co-op students Kevin and Daria.

Last but certainly not the least, I would also like to express my appreciation to my friends and family, whose love and support have been invaluable throughout this process. Thank you for always encouraging me to achieve my goals and reminding me that anything is possible if you put your mind to it.



**TABLE OF CONTENTS**

<b>ABSTRACT</b>	<b>iii</b>
<b>ACKNOWLEDGEMENTS</b>	<b>iv</b>
<b>TABLE OF CONTENTS</b>	<b>v</b>
<b>LIST OF FIGURES</b>	<b>vi</b>
<b>LIST OF TABLES</b>	<b>x</b>
<b>1. INTRODUCTION</b>	
1.1 General	1
1.2 Model System	6
1.3 Apoptosis	9
1.4 $\gamma$ H2AX	12
1.5 Dicentrics	13
1.6 Adaptive Response	17
<b>2. METHODS</b>	<b>19</b>
2.1 Patient Consent and Sample Collection	19
2.2 Irradiation	20
2.3 Apoptosis	21
2.4 DNA Double Strand Breaks	22
2.5 Chromosome Aberrations	23
2.6 Statistical Analysis	25
<b>3. RESULTS</b>	<b>27</b>
3.1 Apoptosis	27
3.2 DNA Double Strand Breaks	31
3.3 Chromosome Instability	35
<b>4. DISCUSSION</b>	<b>41</b>
<b>5. CONCLUSION</b>	<b>64</b>
<b>6. REFERENCES</b>	<b>67</b>
<b>7. APPENDIX</b>	<b>75</b>

## LIST OF FIGURES

Figure 1.1	Percentage Distribution of Diagnostic Imaging Examinations in Hospitals, Canada, Excluding Quebec, 2005-2006 <i>Taken from Medical Imaging in Canada 2007, Canadian Institute for Health Information.....</i> 2
Figure 1.2	Testing Rate per 100,000 Population for CT Exams by Anatomical Site, Ontario, 2005-2006. <i>Taken from Medical Imaging in Canada 2007 Canadian Institute for Health Information.....</i> 3
Figure 1.3	Flow cytometry dot plot of Side Scatter (SS) vs. Forward Scatter (FS). Each dot represents a particle, in this case a mononuclear cell, as it is detected upon interrogation. The black line is the gate (named ‘A’) created around the dots of interest which are presumed to be lymphocytes based on their FS and SS pattern. The gate dictates which cells are to be further analyzed based on fluorescence.....8
Figure 1.4	Figure 1.4: Isolation of peripheral blood mononuclear cells after centrifugation. A) Plasma B) Buffy coat – mononuclear fraction C) Histopaque D) Red blood cells.....8
Figure 2.1	Flow chart of logistics throughout the study.....26
Figure 3.1	Percent apoptosis in human lymphocytes following CT scan. Error bars for each patient represent standard error in 3 flow trials.....28
Figure 3.2	Percent apoptosis in human lymphocytes following 0 and 8 Gy.....29
Figure 3.3	Percent apoptosis in human lymphocytes following CT scan and 8 Gy <i>in vitro</i> challenge dose.....30
Figure 3.4	An overview of the percent differences in apoptosis in lymphocytes of all 8 patients before and after CT (blue) and before and after 8 Gy <i>in vitro</i> (red).....31
Figure 3.5	Gamma H2AX phosphorylation in human lymphocytes as measured by fluorescence intensity following CT scan.....32

Figure 3.6	Gamma H2AX phosphorylation in human lymphocytes as measured by fluorescence intensity following 8 Gy in vitro challenge dose.....	33
Figure 3.7	Graph showing relationship between level of H2AX phosphorylation and DLP values for pelvic CT.....	34
Figure 3.8	Gamma H2AX phosphorylation in human lymphocytes as measured by fluorescence intensity following CT scan and 8 Gy in vitro challenge dose.....	35
Figure 3.9	Dose-response for curve for dicentrics at 0, 2, and 4 Gy gamma rays. Each point represents the average of three volunteers (two male, one female).....	36
Figure 3.91	Microscopy images of metaphase spreads. Top L) Normal met with 46 chromosomes and no apparent aberrations present. Top R) Taken from a 3 Gy sample, note the presence multiple dicentrics with corresponding acentric fragments within a single metaphase (arrow) Bottom L) Also from 3 Gy. Note presence of tracentrics (arrow). Bottom R) Also from 3 Gy with dicentrics and tricentrics present.....	38
Figure 3.92	Frequency of dicentrics in whole blood following 3 Gy <i>in vitro</i> .....	39
Figure 3.93	Frequency of dicentrics in human lymphocytes following CT scan and 3 Gy in vitro challenge dose.....	39
Figure A-1:	Percent contribution of CT scan types to total number of scans (67 million) in 2006.....	76
Figure A-2:	In normal cells (A) there is an asymmetry in the cell membrane and phosphatidylserine is typically located on the inner leaflet (bottom layer). In apoptotic cells (B) PS is externalized on the outer leaflet (top) of the membrane and can be detected by Annexin V (Purple.....	77
Figure A-3:	Steps in the formation of a dicentric chromosome. The interaction of the cell nucleus with energy from ionizing radiation can produce genomic lesions. If breaks occur in two separate pre-replication or G <sub>1</sub> chromosomes (A), they as well as their corresponding broken DNA fragments can join.	



When replication occurs in the S phase (B), there now exists two sister chromatids that also join at the sticky ends, forming a grossly distorted chromosome with two centromeres. Under a microscope (C) the dicentric and their acentric fragments (chromosomes with no centromeres), indicated by the red arrows, are scored within each metaphase.....78

- Figure A-4: DNA strand breaks produced by ionizing radiation and other genotoxic agents can be immediately detected by members of the Phosphatidylinositol 3-kinase-related kinase (PIKK) family (ATM, ATR and DNA-PK) as well as other sensor proteins. ATM in particular undergoes autophosphorylation (P) and subsequently phosphorylates the histone protein H2AX at amino acid Ser-139. Formation of  $\gamma$ -H2AX by this phosphorylation event is required for the recruitment of DNA repair factors such as 53BP1 and BRCA1. 53BP1 also functions to couple ATM with additional downstream targets including p53. The primary outcome of this pathway is damage repair, however the cell can also undergo apoptosis following  $\gamma$ -H2AX induction.....79
- Figure B-1: Dose rate map for the Taylor Radiobiology Facility Cs<sup>137</sup> gamma ray source at McMaster University. Updated April 2010.....80
- Figure B-2: Irradiation set-up at the Taylor source. For apoptosis and  $\gamma$ -H2AX, isolated lymphocytes in supplemented media were aliquoted into duplicate T25 flasks (Left) and irradiated on ice 44.29 cm (dose rate = 0.1 Gy/min) from the opening of the Cs<sup>137</sup> source. For the dicentric assay, 0.5 ml of whole blood was irradiated in flat-side tubes (Right) at room temperature 44.29 cm from the opening of the source.....81
- Figure B-3: Dot plots of controls from Annexin-FITC/7AAD apoptosis assay. Isolated lymphocytes were adjusted to  $5 \times 10^5$  cells/ml and labeled with either Annexin only (A), 7AAD only (B) and an unstained control (C) prior to flow analysis. Annexin was analyzed for green fluorescence (FITC – green dots) and red fluorescence (7AAD – red dots). Blue dots indicate those cells that are negative for both Annexin and 7AAD (bottom left quadrant). L Panel: Lymphocytes gates on forward scatter (FS) and side scatter (SS) patterns. R Panel: Percentage of Gate A that is positive for Annexin V.....82

Figure C-1: Percent apoptosis results from sham CT control experiment. Lymphocytes that were collected before and after sham CT were also irradiated *in vitro* with 8 Gy apoptosis was compared before and after treatment.....84



## LIST OF TABLES

Table 1.1	Average number ( $N$ ) of metaphases scored for each treatment.....	16
Table 2.1	CT details for patient volunteers.....	20
Table 3.1	Apoptosis measured in human peripheral blood lymphocytes isolated from blood taken before and after a CT scan with 0 and 8 Gy gamma <i>in vitro</i> challenge doses.....	29
Table 3.2	Levels of phosphorylated histone H2AX as measured by mean fluorescence intensity in human peripheral blood lymphocytes before and after a CT scan with 0 and 8 Gy gamma <i>in vitro</i> challenge doses.....	33
Table 3.3	Frequency of dicentrics per cell for each patient with average values for each treatment.....	37
Table C-1:	Comparison data for all patients. These tables show the percent difference following different radiation treatments. A) Difference before and after CT B) Difference before and after 8 Gy <i>in vitro</i> C) Difference between 8 Gy only (left) and 8 Gy following CT scan (right). For all tables, negative values indicate a decrease before and after.....	83

# **1. INTRODUCTION**

## *1.1 GENERAL*

The clastogenic effects of ionizing radiation (IR) have made it a primary candidate for cancer therapy, as well as a major concern for human health. The ironic interplay between damage and protection which defines the many roles of radiation in medicine and safety regulations has prompted the ongoing investigation of the molecular mechanisms that govern biological changes following exposure. The need for understanding how radiation affects living things by both the scientific and public communities grows as the application of radiation in medicine as well as in other areas such as energy production continues to advance.

More than half of the radiation we are exposed to in our lifetime comes from natural sources such as radon gas, cosmic, terrestrial, and our own bodies. The remaining portion is from man-made sources including consumer products, nuclear medicine and various x-ray medical imaging modalities such as mammograms and computerized tomography (CT) scans [1].

According to the World Health Organization, approximately 20-30% of medical cases worldwide require the use of diagnostic imaging [2]. Although the majority of problems are resolved using basic x-ray and/or ultrasound examinations, CT scan use was reported to comprise about 12 percent of medical exams in Canada in 2006, which is double the use of nuclear medicine and magnetic resonance imaging technology (Figure 1.1) [3]

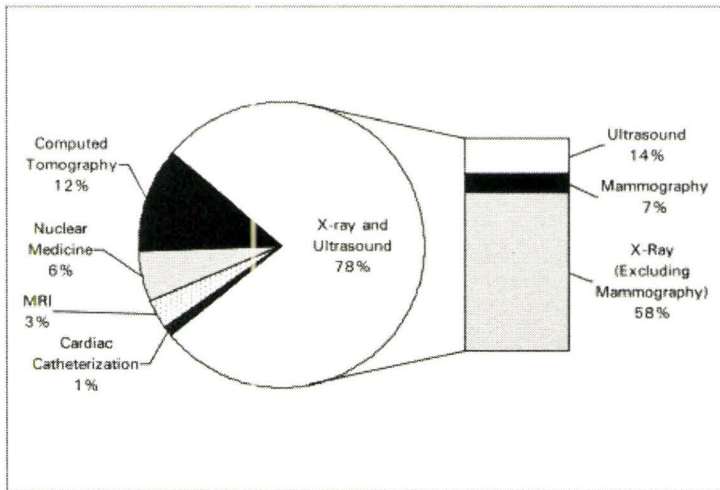


**Figure 1.1: Percentage Distribution of Diagnostic Imaging Examinations in Hospitals, Canada, Excluding Quebec, 2005-2006 Taken from *Medical Imaging in Canada 2007*, Canadian Institute for Health Information<sup>3</sup>**

The CT, which was first introduced in the 1970s, has become an important tool in the diagnosis of medical conditions and, in the case of this study, the identification and evaluation of cancer progression. In 2005, over a million Canadians aged 15 and over reported having gone for a CT scan in the past year. At that time brain CTs were most common in emergency scenarios; however the most frequent CT scan for inpatients was performed on the abdomen or pelvis (Figure 1.2) (Also see Figure A-1 in APPENDX A) [3].

Accurate localization of prostate cancer is crucial for treatment, and current methods for detection and staging such as measuring circulating serum prostate specific antigen (PSA) have not been as successful as *in vivo* imaging techniques in tumour characterization [4]. Patients in this study have been diagnosed with carcinoma of the

prostate and must go through a routine pelvic CT for appropriate treatment planning and patient management prior to radiation therapy.

In general, CT scans operate by producing high resolution images of internal anatomical and physical structures in order to aid health professionals in the identification and treatment of conditions relating to trauma, inflammation and cancer [5]. Unlike medical x-rays, CT is enabled by advanced software that forms 3-dimensional projections from hundreds of 2-dimensional slices. Advancements in CT technology - which have lead to faster rotation times, accelerated computing power and multi detectors that produce smaller slices with larger coverage - have contributed to its efficiency and preferred use against alternative diagnostic methods [6].

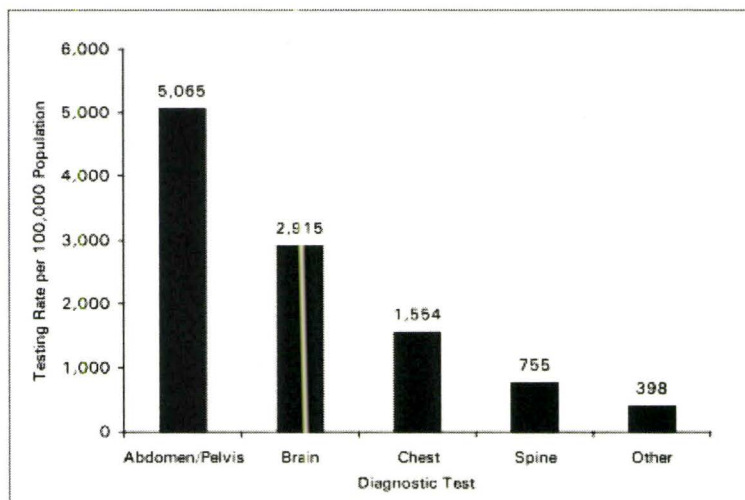


**Figure 1.2: Testing Rate per 100,000 Population for CT Exams by Anatomical Site, Ontario, 2005-2006. Taken from *Medical Imaging in Canada 2007* Canadian Institute for Health Information<sup>3</sup>**

Alongside the expanding use of modernized CT technology is the growing concern for the increase in radiation over-exposure and possible risk for stochastic effects, mainly cancer. Although the dose to patients has been greatly reduced over the years, some research still predicts, using models, a possible increase in cancer risk following one or multiple CT scans, especially in children [7,8]. This brings attention to the linear, non-threshold (LNT) model for radiation associated cancer risk which estimates that the deposition of energy from IR increases cancer risk linearly with increasing dose. Epidemiological studies examining cancer rates in populations that were exposed to large, acute doses of radiation, such as the atomic bomb survivors, prompted some researchers to extrapolate data to the lower end of the dose spectrum. Although this linear model seems convenient for the establishment of international regulations for radioprotection, it is constantly challenged by molecular and animal studies that show a different relationship between low dose radiation and high dose induced-carcinogenesis.

For decades radiobiological studies have observed responses to radiation at the cellular and physiological level. Essentially, radiation induces its effects mainly through DNA damage, which is a well accepted and proven notion [9-11]. Being the principle target of radiation, DNA can acquire a variety of lesions that, depending on the type and level of damage, can result in outcomes such as DNA repair, apoptosis, necrosis, or mutation and carcinogenesis. Modest doses of low linear energy transfer (LET) radiation can produce single strand breaks that are quickly repaired and thus usually have little biological consequences [12]. Complex DNA double strand breaks (DSBs) and locally multiply damaged sites (LMDS) are more difficult to repair [9] and may contribute to



mutagenesis and cancer after radiation over-exposure. These lesions can be produced by IR directly (such as in the case of particulate radiation and seldom in photon radiation), or indirectly through the interaction of DNA with free radical products of radiolysis and lipid oxidation at the cell membrane [12, 13]. Although it is logical to argue that, given the known interactions between energy deposited from an IR track and biological molecules, even the smallest dose of radiation can produce damage, it is also known that cells are able to respond through a variety of pathways and eliminate the damage. Mechanistic studies have elegantly illustrated the ability to attend to DNA damage through repair pathways, or eliminate damage through apoptosis. Studies have also shown that during these responses, there is an upregulation of genes involved in repair, antioxidant defenses [14], and intercellular communication [15]. These observations again present a challenge to the LNT model of radiation carcinogenesis and promote the ongoing investigation of biological changes following low-dose radiation which includes radiation from diagnostic imaging. Apoptosis, DNA damage, and chromosome aberrations are all induced and modified by radiation [11]. These endpoints are also the primary areas of interest for the following experiments.

Overall, the purposes of this study are:

- To measure biological changes in peripheral lymphocytes following *in vivo* irradiation by a pelvic computerized tomography scan
- To examine the degree of inter-individual differences in radiosensitivity and compare these results to previous work

- To determine whether or not lymphocytes are able to exhibit an adaptive response with regards to cell death, chromosome aberrations and DNA damage
- To observe the sensitivity of these endpoints to doses delivered from a CT scan

It is hypothesized that there will be a high degree of inter individual variability in radiation responses between patients undergoing a CT scan for radiotherapy planning. The null hypotheses are 1) that there will be no significant increase or decrease in apoptosis, levels of chromosome aberrations and DNA damage in peripheral blood lymphocytes following a computerized tomography scan and 2) that there will be no change in cellular response (adaptive response) shown in CT exposed samples after the lymphocytes are challenged with a large radiation dose.

### *1.2 MODEL SYSTEM*

Human peripheral blood lymphocytes were used to elucidate the biological effects of low dose radiation. Lymphocytes are a subpopulation of white blood cells that are responsible for identifying and killing pathogens during the adaptive arm of the immune response. These cells are predominantly non-dividing and thus they are an ideal cellular model system due to their synchronicity. This helps eliminate cell cycle stage as a variable in any observed changes in radiosensitivity since all cells are irradiated at  $G_0$ . Lymphocytes are an ideal model system to observe radiobiological changes due to the fact that they are easy to obtain, can be processed and analyzed within weeks, and are demonstrated to have a high sensitivity to radiation [12,16,17]. Cell types that regularly undergo division will experience levels of mitotic or post mitotic/reproductive death

following exposure. Alternatively, lymphocytes will undergo interphase death by apoptosis and these cells as well as cells derived from germinal lineages are considered highly sensitive to IR-induced apoptosis [13]. However when undamaged or if the damage is stable, lymphocytes cells can simply reside in the periphery for up to 20 years in adults [18].

For cytogenetic analysis, stimulation into mitosis of naive lymphocytes is required and this was first demonstrated by Nowell using Phytohemagglutinin (PHA) [19]. PHA is a sugar-binding protein derived from the bean plant *Phaseolus vulgaris* which can induce lymphocyte division and transformation into blastoid cells [18, 19]. Lymphocytes normally take 48 hours to undergo a single division under the influence of a mitogen.

Flow cytometry is an application which quantifies levels of fluorescence detected following the interrogation of particles that travel within a stream of fluid and pass through a detector one at a time. Lymphocytes are small with dense nuclei and little surrounding cytoplasm [18]. Their diameter, volume and overall size are well known, thus allowing for rapid experimental analysis when interpreting data by flow cytometry. The forward scatter pattern, which is indicative of cell size, and side scatter pattern, which determines cell granularity, is readily identified during flow set up (Figure 1.3). Current flow cytometry methods for analyzing both apoptosis and  $\gamma$ -H2AX expression have required the prior separation of lymphocytes from the whole blood (Figure 1.4) [20]. Factors sequestered in the plasma such as cytokines, chemokines, and other

mitogens within whole blood can dramatically affect the apoptotic response in lymphocytes during irradiation [21]

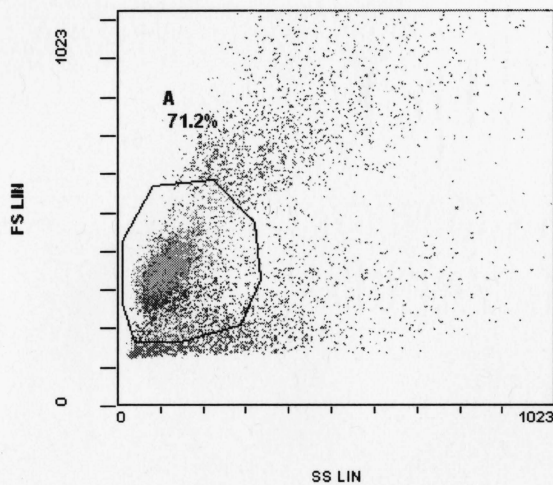


**Figure 1.3: Flow cytometry dot plot of Side Scatter (SS) vs. Forward Scatter (FS). Each dot represents a particle, in this case a mononuclear cell, as it is detected upon interrogation. The black line is the gate (named 'A') created around the dots of interest which are presumed to be lymphocytes based on their FS and SS pattern. The gate dictates which cells is to be further analyzed based on fluorescence**

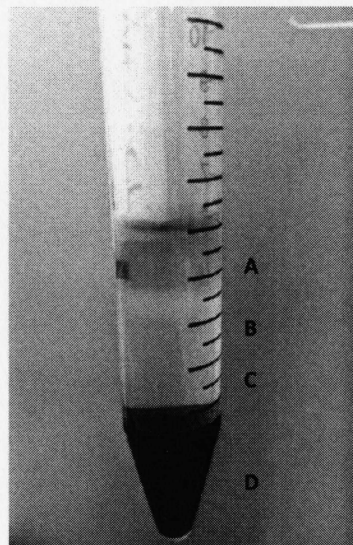


**Figure 1.4: Isolation of peripheral blood mononuclear cells after centrifugation. A) Plasma B) Buffy coat – mononuclear fraction C) Histopaque D) Red blood cells**

### *1.3 APOPTOSIS*

Apoptosis is a genetically controlled, protein-synthesis dependent mode of cell death characterized by a series of morphological and biochemical changes. A highly conserved active process, apoptosis is fundamentally different from necrosis, which is a more passive method of 'cell suicide' [17] marked by complete loss of membrane integrity, aggregation of chromatin and significant inflammatory responses. Apoptosis has been repeatedly observed in metastatic and normal tissue and, in both cases, can be initiated in different cellular components such as the nucleus, cytoplasm, and membrane [13]. Since early experimental observation, the criteria for identification of cells undergoing apoptosis have been well defined, and includes an increase in cellular granularity, cell shrinkage, chromatin condensation, DNA fragmentation into approximately 185 bp segments, membrane blebbing, and formation of apoptotic bodies which are phagocytosed by neighbouring macrophages [22 - 25]. Apoptosis is considered a vital regulatory mechanism that maintains cellular tissue homeostasis and promotes the destruction of unwanted cells during growth and development as well as in differentiation and cell turnover. Both physiological and pathological cues can stimulate a cell into apoptosis, including extracellular stresses such as radiation, heat, and oxidative stress, as well as through external activation by receptor-mediated processes involving death receptors, growth factor withdrawal, cytotoxic lymphocyte activity, and chemotherapeutic drugs [13, 26].



Apoptosis has consistently been implicated in studies evaluating cellular responses to IR. Radiation-induced cell death in both human and murine lymphocytes is a kinetically slow process, triggered by damage to DNA – a critical target which in the case of low LET radiation is typically damaged indirectly by free radical products. Apoptosis following radiation-induced DNA damage shows a similar kinetic profile to apoptosis caused by other DNA damaging agents such as cisplatin and bleomycin [27, 28]. Other evidence still suggests that lipid peroxidation leading to membrane damage caused by IR-produced free radicals may also lead to a similar fate, although membrane oxidizing agents such as t-butyl hydroperoxide initiate apoptosis much quicker, suggesting that a different pathway may be taking place [27]. Despite variations in levels of apoptosis amongst cell types and organisms, overall this endpoint is dose-dependent and as such it has been evaluated as a possible biodosimeter [29] and predictor of cellular toxicity in patients undergoing radiation therapy for cancer treatment [21, 30]. The molecular mechanism of  $\gamma$ - or UV radiation-induced premitotic apoptosis in lymphocytes is triggered by the onset of DNA damage which, if irreparable, may lead to the upregulation of pro-apoptotic factors such as Bax, a protein of the Bcl-2 family, or CD95 death receptor via stabilization of transcription factor p53 [13]. These proteins as well as reactive oxygen species can trigger the mitochondria to release caspase-activating factors. Prompt activation of caspases is an important step in the induction of downstream intrinsic and extrinsic apoptotic pathways, ultimately leading to the removal of the damaged cell [25]

Flow cytometry is a sensitive method for the quantification of apoptosis following exposure of peripheral blood lymphocytes to low dose radiation. Other assays that observe cell death such as fluorescence analysis of DNA unwinding (FADU), *in situ* dUTP nick end labeling [31] and the comet assay are only a few of many methods used to visually observe and quantify apoptosis. However such experiments are time consuming, labour intensive and usually require the loss of cell viability or physical integrity [24]. In response to these drawbacks, flow cytometry has proven to be a rapid, highly specific and cost-effective method for evaluating levels of apoptosis as it targets biological markers that are unique to the apoptotic profile.

An early event of apoptosis is the translocation of phosphatidylserine (PS) on the outer layer of the plasma membrane. (Figure A-2) The loss of membrane asymmetry through externalization of this phospholipid molecule may occur immediately after caspase activation and can be detected by the protein Annexin V, which binds to exposed PS in a calcium-dependent manner [32, 33] (Figure A-2). The high-affinity binding property of Annexin to PS makes it a favourable candidate for flow cytometric studies. It is typically conjugated with Fluorescein isothiocyanate (FITC), a molecular fluorophore with an absorption and emission maximum of 495nm and 520nm respectively. Together with DNA viability dye 7-Aminoactinomycin D (7-AAD), Annexin-FITC can rapidly detect cells in the early apoptotic stage.

Previous experiments by Boreham *et al.* which looked at the kinetics of radiation-induced apoptosis noticed a slow reaction *in vitro*, reaching a maximum at about 72 h

post exposure to low dose  $\gamma$ -rays [29]. The largest increase in apoptosis took place between 48 and 72 hours. Based on this it was determined that in order to observe and measure the frequency of lymphocytes in the early apoptotic, pre necrotic stage, flow cytometric analysis needed to be taken place after an approximately 40-45 h incubation period.

#### 1.4 $\gamma$ -H2AX

H2AX is a member of the histone sub-family H2A, one of five which constitute the proteins around which eukaryotic DNA is packaged and organized. Approximately 140 bp of DNA coil around a core of eight histones, forming a nucleosome. In lymphocytes, histone H2AX constitutes about 2% of total H2A found in the chromatin [34]. These proteins play an important role in the initiation of DNA DSB repair, which is marked by the phosphorylation of H2AX at on serine-139 located at the C-terminus, by PI3K-like kinases including ataxia telangiectasia mutated (ATM), ataxia telangiectasia and Rad3-related (ATR) and DNA-dependent protein kinases (DNA-PK) [34-36] (Figure A-3). The formation of  $\gamma$ -H2AX occurs and can be detected within minutes of DSB induction [36, 37]. This step is essential for the recruitment of repair factors to the site of damage [20] and thus loss or impairment of this process has been linked to carcinogenesis.  $\gamma$ -H2AX has become a sensitive marker for assays measuring the induction of DSBs [37] and its detection may be useful in identifying precancerous cells as well as radiosensitivity of tumour and normal tissue [34].

Although thousands of H2AX histones are phosphorylated following DSB formation, the process is transient and as breaks are repaired, foci slowly disappear. This places a limitation on assays that measure H2AX formation in order to assess radiation-induced DNA damage as samples must be processed right away to accurately assess radiation-induced damage. Löbrich *et al* performed a study to evaluate radiosensitivity *in vivo* following CT scans based on  $\gamma$ -H2AX. Results show that levels of phosphorylation increased linearly with increasing DLP values [37], which was also observed in CT studies conducted in our lab. This and other published studies confirmed that  $\gamma$ -H2AX levels are highest 0.5 h post irradiation within the 0-10 Gy dose range, and slowly begin to decrease after that time [20].

The high throughput of data using flow cytometry has made it an ideal candidate to enumerate  $\gamma$ -H2AX in order to determine levels of DNA DSBs in peripheral blood lymphocytes.

### 1.5 DICENTRICS

Radiation-induced chromosome aberrations have been extensively observed for decades, with effects described in terms of structural changes that result from rearrangement of broken ends formed from unrepaired DNA double stranded breaks. Dicentric chromosomes, in particular, have proven to be valuable and reliable biomarkers for radiation damage. Chromosome aberrations are classified on the basis of their process of formation [38]. Chromosome-type aberrations, which are typically associated with IR, are produced when cells are irradiated prior to the S phase of the cell cycle. Breaks that

occur in single-stranded chromatin are thus reproduced in the complementary strand during DNA replication and are visible on both sister strands during mitosis [12].

Dicentrics are chromosome-type aberrations produced when two pre-replication chromosomes in close proximity with double stranded breaks form an illegitimate union. The fused chromosomes and their corresponding leftover fragments are replicated during S phase, resulting in a morphologically distorted chromosome containing two centromeres with accompanying acentric fragments [12] (Figure A-4).

The Dicentric Assay (DCA) is used for biodosimetric analysis and clinical triage [39] following radiation accidents or incidents where physical dosimeters are not present to monitor the dose to exposed individuals. Dicentrics are highly IR-specific (natural background frequency of ~1-2 in 1000) and dose dependent. In 2004, the International Organization for Standardization (ISO) produced a guideline outlining laboratory practices for scoring dicentrics, recognizing this assay [40] as an international ‘Gold Standard’ [39].

Proper execution of the Dicentric Assay and other cytogenetic preparations requires the artificial induction of cell proliferation of lymphocytes which are normally quiescent. Several mitogens are commercially available and are potent in their ability to stimulate lymphocyte division. Most studies use phytohaemagglutinin (PHA), a plant lectin widely used for the DCA [18]. Lymphocytes require approximately 48 hours to undergo division, and so in many experiments samples are cultured for 44-48 hours in the presence of PHA. Chromosomes are highly condensed and thus best observed during the



metaphase step of mitosis. In order to arrest cells at this stage an additional 2 hour incubation period in the presence of colcemid is also required. Colcemid acts as an arresting agent by inhibiting the polymerization of microtubules which comprise the mitotic spindle. Chromosomes are therefore no longer able to attach to spindle fibres which they use to migrate to opposite poles during anaphase.

Unstable aberrations result in a loss of genetic material in the subsequent mitosis. In order to acquire a proper dose estimation, cells must only be scored in the first division after exposure. The use of colcemid and strict incubation time normally prevent cells from continuing through the cell cycle, but there still remains a small population that do so. This poses limitations in dicentric scoring as damage incurred will be diluted in the following division. To avoid this, a fluorescence plus Giemsa (FPG) technique is employed using bromodeoxyuridine (BrdU), a synthetic thymidine analogue that is taken up during DNA replication. After the second division, one sister chromatid will be unifilarly labeled while the other bifilarly labeled. The chromatid with two BrdU labeled strands will not be stained, producing a 'harlequin' effect in the metaphase chromosomes [18]. Hoechst is a DNA-binding fluorescent stain excited by UV light. When incorporated into culture, BrdU and Hoechst allow for rapid detection of cells in their second division (M2) [18].

Dose-response curves for dicentrics are typically derived from information from 1000 metaphases, however due to time and volume of data in this study approximately 100-200 metaphases were scored for each treatment (Table 1.1). Although large numbers

of cells are available for scoring at lower doses and the greater the number of cells scored the greater the statistical significance, the International Atomic Energy Agency (IAEA) states that dose estimation and damage detection is still possible with 200 metaphases [18].

**Table 1.1 – Average number (*N*) of metaphases scored for each treatment**

<b>Treatment</b>	<b>Average <i>N</i></b>
Pre 0 Gy	177
Post 0 Gy	169
Pre 3 Gy	126
Post 3 Gy	111

Being the standard for biodosimetry and clinical triage situations [39], the Dicentric Assay has been repeated in many labs with results that are consistent with current dose response curves. Established scoring criteria will yield data regarding frequency of dicentrics, acentric fragments, and rings [18] which are another type of lethal aberration formed when two breaks in the same pre-replication chromosome lead to the joining of sticky ends [12]

Dose response curves possess different shapes and slopes that can vary depending on LET and dose-rate [38]. Due to small differences between yield curves of x and  $\gamma$ -rays, it is suggested that an appropriate calibration curve is produced for the specific radiation used. A large body of evidence shows that the, for low LET radiation, the relationship between the frequency of dicentrics and dose is best fitted by a linear quadratic model with the following equation:

$$Y = A + \alpha D + \beta D^2$$

Where D = Dose and Y = dicentric frequency

### *1.6 ADAPTIVE RESPONSE*

The adaptive response is a biological phenomenon defined by the reduced effect of a large ‘challenge dose’ of radiation following exposure to a smaller, ‘priming dose’ of radiation. This protective response has been observed using different biological endpoints such as: cell death, chromosome aberrations, mutation induction, clonogenic survival, micronuclei, cancer latency, and DNA repair [41-47]. In addition, the effect is not limited to radiation, but can also be caused by other chemical or genotoxic agents such as bleomycin, hydrogen peroxide, hyperthermia, and restriction enzymes [28, 44, 47, 48]. Radiation-induced adaptation is a concerted effort of extracellular signals and intracellular responses [15] that can occur following exposure to both low LET ( $\gamma$ -rays, x-rays, beta) and high LET (alpha particles, neutrons) radiation [49]. Suggested mechanisms which lead to cellular adaptation include the upregulation of antioxidant defenses and an accelerated repair response [41]. For decades it was accepted that only cells which were directly traversed by radiation were subject to intracellular responses that lead to an adaptive response, but recent evidence shows that non-targeted cells may also adapt if in close proximity with cells that have been directly hit. The mechanism responsible for this and other related phenomena such as the maintenance of the adaptive response in human cells from a few hours to several months is still in question [15].

Adaptation in human lymphocytes by IR was first reported in 1984 by Olivieri and Wolff [46]. Their work illustrated the effect of chronic exposure to continuous low doses of radiation by incorporating tritiated thymidine (3H-TdR, a radiolabeled nucleoside) into cells prior to irradiation with a large x-ray challenge dose. They discovered that the combined effect of 3H-TdR and x-rays on the frequency of chromosome aberrations was significantly lower than that of x-rays alone.

Studies which ensued observed the adaptive response in populations exposed *in vivo* to occupational levels of radiation [50] or who experience very high levels of natural background radiation in areas such as Iran, where individuals can receive an annual absorbed dose up to 260 mSv y<sup>-1</sup> [51]. Furthermore, many molecular studies demonstrating radioadaptation have looked at a variety of bioindicators of genetic damage in cell types including nondividing lymphocytes and fibroblasts.

The following study will determine whether or not the dose delivered from the CT scan will induce an adaptive response in the peripheral blood lymphocytes of the patient volunteers. In terms of apoptosis, a cell undergoes programmed cell death following genotoxic stress to confer protection to the organism from genetic risk [74]. Thus, if the lymphocytes are able to adapt following the ‘priming’ CT dose, they should show decreased apoptosis in response to the 8 Gy *in vitro* challenge dose.

## 2. METHODS

### 2.1 *PATIENT CONSENT AND SAMPLE COLLECTION*

The study accrued 8 patients between the ages of 62 and 77 who are currently being treated at the Juravinski Cancer Centre in Hamilton for adenocarcinoma of the prostate. The protocol outlining this study was approved by the Hamilton Health Sciences Research Ethics Board and a consent form informing the patients of the study was signed by each patient.

Patients were then scheduled for a CT scan as part of their planning for radiotherapy. Blood samples (10 ml) were taken directly before and after the scan was performed. Each 10 ml sample of blood was collected by venipuncture and kept in sodium heparin collection tubes (Vacutainer, BD Biosciences, Mississauga, ON, Canada). The tubes were packaged in bubble sleeve wrap and biohazard bags and delivered at room temperature for further processing with an average elapsed time of 3 h between the first sample collection and processing.

Isolation of lymphocytes from the whole blood required the use of a density gradient cell separation medium. About 3 ml of blood from pre- and post-CT samples were gently and aseptically layered onto 3 ml of Histopaque-1077 in conical tubes (15 ml). Tubes were centrifuged at room temperature for 30 min at 300g as per the manufacturer's instructions (Sigma-Aldrich, Oakville, ON, Canada). Mononuclear fractions containing the lymphocytes were isolated and washed once with PBS and once with complete RPMI (16 % Fetal Bovine Serum, 0.8% L-glutamine, 0.8% Penicillin

Streptomycin). Cell concentrations were quantified using a Z2 counter (Beckman Coulter, Mississauga, ON, Canada) and adjusted to  $4-5 \times 10^5$  cells/ml with RPMI. After proper adjustment of cell concentration, 4 ml of sample was placed into appropriately labeled T25 flasks (BD Falcon™, BD Biosciences, Mississauga, ON, Canada) and placed on ice in a styrofoam insulator.

## 2.2 IRRADIATION

### 2.2.1 Computerized Tomography Scan

Patients were imaged with a GE Lightspeed RT multislice helical scanner (120 kV). Scans typically took 20-30s and images were acquired in axial mode with a slice thickness of 2.5 mm for all patients. One male volunteer was used for a sham CT control.

**Table 2.1: CT details for patient volunteers**

<u>Patient</u>	<u>Initials</u>	<u>Date of Scan</u>	<u># of Scans</u>	<u># of Slices</u>	<u>Slice Thickness (mm)</u>
1	J-H	Jun-22	1	No data	2.5
2	V-B	Jul-12	2	127	2.5
				122	2.5
3	M-C	Aug-10	3	123	2.5
4	H-V	Aug-17	2	118	2.5
				116	2.5
5	G-B	Aug-23	1	125	2.5
6	W-W	Aug-24	1	131	2.5
7	J-G	Aug-24	1	131	2.5
8	P-H	Aug-30	1	129	2.5



### 2.2.2 Irradiation Challenge

All challenge dose irradiations were done using a  $^{137}\text{Cs}$  source (662 keV) at dose rate of 0.1 Gy/min. The distance required to maintain this rate was calculated using the most recent decay equation (Refer to Figure B-1):

$$y = 14.14x^{-0.551}$$

Mononuclear cells in supplemented RPMI held at 0°C in ice slurry were irradiated with 8 Gy for the Apoptosis and H2AX assays, whereas for the dicentric assay whole blood was irradiated with 3 Gy at room temperature. Control samples were sham-irradiated (Figure B-2).

### 2.3 APOPTOSIS

Levels of cell death were measured using the Annexin V- Fluorescein Isothiocyanate /7-Amino-Actinomycin D (Annexin V FITC/7AAD) flow-based assay. Following high dose gamma- irradiation, T25 flasks containing pre and post-CT exposed mononuclear cells in supplemented RPMI were transported on ice to the radiobiology lab and placed in a 5% CO<sub>2</sub> incubator (95% relative humidity, 37°C) for 44 h. After incubation, 500ul was aseptically transferred from T25 flasks into labeled 5 ml flow tubes. Samples were prepared in triplicate. The tubes were spun at 300g for 5 minutes and the supernatant was decanted. An antibody cocktail containing Annexin and viability dye 7AAD (Beckman Coulter #FI08016) was prepared and 100ul of the cocktail was added to each sample. Controls were also prepared as followed: Annexin (5ul) only,

7AAD (10ul) only and one tube was kept unstained. Samples were then incubated for 15 minutes on ice and given 300ul of binding buffer prior to cytometric analysis using a Beckman Coulter EPICS XL Flow Cytometer (Beckman Coulter, Mississauga, ON, Canada). Control tubes were tested for each patient to ensure gates were set appropriately (Figure B-3). Lymphocytes were gated based on forward scatter vs. side scatter properties (Figure 1.3), and the percentage of cells positive for Annexin as determined by fluorescence was quantified. Information was collected from 10,000 lymphocytes and the average of 3 trials was recorded.

#### *2.4 DNA DOUBLE STRAND BREAKS*

DNA double strand breaks were assessed using the H2AX assay. After irradiation with 8 Gy challenge dose, flasks containing pre and post-CT samples were brought back to the radiobiology lab and aseptically transferred into labeled flow tubes set aside for this part of the experiment (500ul/tube). The tubes were then incubated in a water bath set to 37°C for 0.5 h. Samples were then fixed with 3ml of ice cold 70% ethanol and placed on ice for 30-60 minutes before storage at -20°C.

Before analyzing samples on the cytometer, tubes were centrifuged at 300g for 8 minutes. The supernatant was aspirated and the pellet was resuspended in 3ml of 1x Tris-Buffered Saline (TBS, Ph 7.4). They were then re-centrifuged for an additional 8 minutes and supernatant was aspirated before addition of 1ml cold, freshly prepared Tris-Saline-Triton (TST) (96% 1x TBS, 4% Fetal Bovine Serum, <1% Triton X-100). Samples were incubated with TST for 10 min on ice, and then centrifuged at 300g for 8 minutes. Each

tube was stained with 100ul of antibody cocktail consisting of TST (100ul/tube) and Alexa Fluor 488 mouse anti-human H2AX antibody (BD Pharmingen #560445, 3ul/tube). Tubes were gently mixed by vortex and incubated on ice for 40 min – 1 h. After incubation, samples were washed in 2 ml TST and labeled with 300ul of a TBS/Propidium Iodide (PI) solution (20ml 1x TBS, 333ul of PI) to ensure cells were at the G<sub>0</sub> phase of the cell cycle. Samples were kept on ice and analyzed on the cytometer directly after. Mean fluorescence intensity values were measured and the average of 2 trials for each treatment was recorded.

## *2.5 CHROMOSOME ABERRATIONS*

Levels of chromosome damage were measured using the dicentric assay. Immediately post CT scan, 0.5 ml of whole blood was transferred into 15ml flat-sided tubes in duplicates and irradiated up to 3 Gy at room temperature. Complete RPMI (16 % heat activated Fetal Bovine Serum, 0.8% L-glutamine, 0.8% Penicillin Streptomycin) was pre-warmed to 37°C and added to each tube after irradiation up to 5 ml. To stimulate division, 90ul of Phytohemagglutinin was added. To identify and score cells in the first mitosis (M1), 23ul of 5-bromo-2-deoxyuridine/BrdU (Sigma #B9285) was also added. Samples were incubated at 37°C under 5% CO<sub>2</sub> and 95% humidity for 44 h. After this period, 50ul of 10ug/ml colcemid KaryoMAX® Colcemid™ Solution, #15210-040) was added and samples were incubated for an additional 2 h to facilitate metaphase arrest.

After incubation, samples were centrifuged at 200g for 8 min at room temperature and the cell pellet was isolated and resuspended. To promote cell swelling, 5 ml of

hypotonic KCL was gently added and samples were kept in a 37°C water bath for 15 min. A soft fix was performed by adding 1 ml of freshly prepared ice 3:1 cold fixation solution (3 methanol: 1 glacial acetic acid) was added to each tube and samples were centrifuged at 200g for 8 min (5°C). The supernatant was aspirated and cell pellets were resuspended with 10 ml of 3:1 fixative solution. The fix was repeated two more times with 10 minute incubations on ice in between. Samples were stored at -20°C until ready for slide making.

Metaphase spreads were prepared manually using fresh 3:1 or 2.5:1 fixation solution. Clean slides were kept in 50 ml Coplin jars containing fresh methanol and taken out only when ready for slide making. Once slides were removed, they were wiped clean using KimWipes and 1-2 drops of sample were placed onto the slide using disposable pasteur pipettes. Fixative was flushed over the sample and slides were air dried using manual techniques and a slide warmer set to 40-50°C. Mitotic index and degree of chromosome spreading was evaluated using a light microscope.

Slides were stained first with Hoechst solution (800 of 1 mg/ml Hoechst (Sigma #B2883) in 40 ml distilled H<sub>2</sub>O for 2 minutes, followed by the addition of 110ul Na<sub>2</sub>HPO<sub>4</sub>. Slides were cover slipped, placed on a slide warmer set to 60°C and exposed to UV light for 4 minutes. They were then washed with dH<sub>2</sub>O and placed in a Coplin jar containing 10% Giemsa (4 ml Giemsa (Sigma #GS500) in 36 ml buffer solution (EMD, R0S003/01 pH 6.8) for 10 min. Giemsa solution was rinsed off with dH<sub>2</sub>O and buffer solution, and slides were dried on a slide warmer set to 37°C for a few hours up to

overnight. Cover slips were mounted over each slide and metaphases were analyzed using an Olympus BX51 multi-purpose microscope (100x magnification). Approximately 150-200 metaphases were scored for samples which showed a higher mitotic index and about 80-100 metaphases were scored for samples which showed a lower m-index.

Dicentrics, acentric fragments, and rings were scored.

## *2.6 STATISTICAL ANALYSIS*

The average of each treatment and for each patient was also calculated and plotted in each corresponding graph. To determine significance, a student's T-test was performed to determine the p-value for changes before and after CT, as well as for the adaptive studies. For dicentrics, the p-value was calculated using Fisher's Exact Test



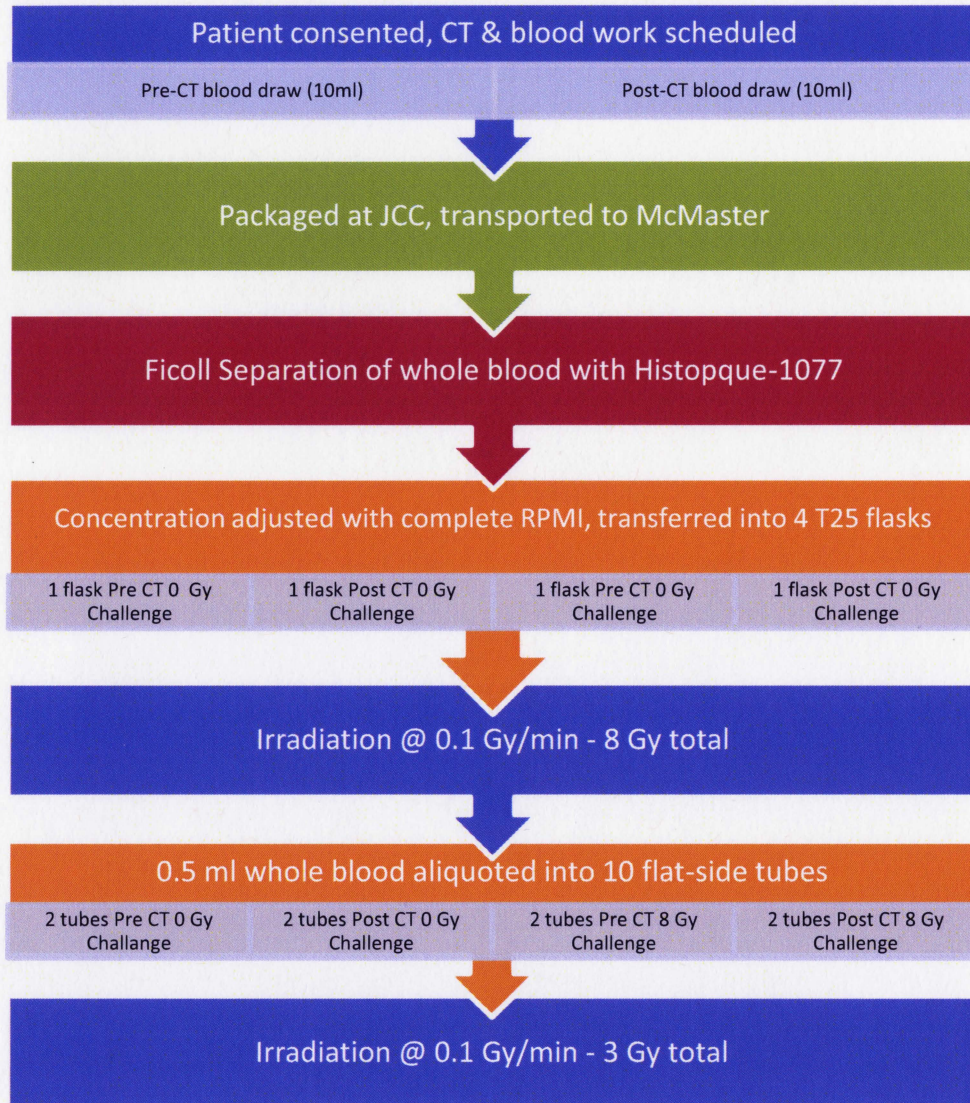


**Figure 2.1: Flow chart of logistics throughout the study**



### 3. RESULTS

#### 3.1 APOPTOSIS

##### ***Inter-individual variability in lymphocyte apoptosis is seen following pelvic CT scan and 8 Gy exposure in vitro***

Variability in apoptotic responses following CT irradiation was observed (Figure 3.1). Four of the eight patients displayed an increase in apoptosis, with Patient 1 showing significant increase. Three patients displayed a decrease in apoptosis, and only one patient stayed the same. Flow cytometric analysis of lymphocytes gated based on their forward and side scatter patterns were Annexin V<sup>+</sup>/7AAD<sup>-</sup>, suggesting that these cells are in the early apoptotic, pre-necrotic phase of cell death. Overall, when frequency of apoptosis was averaged for all patients there was no significant increase or decrease following the CT scan. The largest differences were seen in Patient 1 who had an increase in apoptosis of ~8%, and Patient 5 experienced a decrease of ~13% following CT. The error bars represent error three flow cytometry trials for each patient and treatment (pre CT, post CT). Table C-3 outlines percent differences in all patients. Figure 3.1 also shows spontaneous levels of apoptosis for all patients (black bars). This is seen in lymphocytes isolated from blood collected before the CT scan, and is thus not treated. There is considerable variation in baseline levels of cell death, and different relationships were observed between spontaneous levels and level of increase or decrease in lethality following a CT. To determine whether differences in apoptosis were due to other variables such as the time lapse between the pre and post sample collection (~1 h) or a

noise signal from flow cytometry, a sham CT experiment was conducted in a male volunteer within the same age range as the patients. The results show that the level of apoptosis did not change before and after the CT, and the spontaneous level was also close to what was observed in the patient volunteers (Figure C-1).

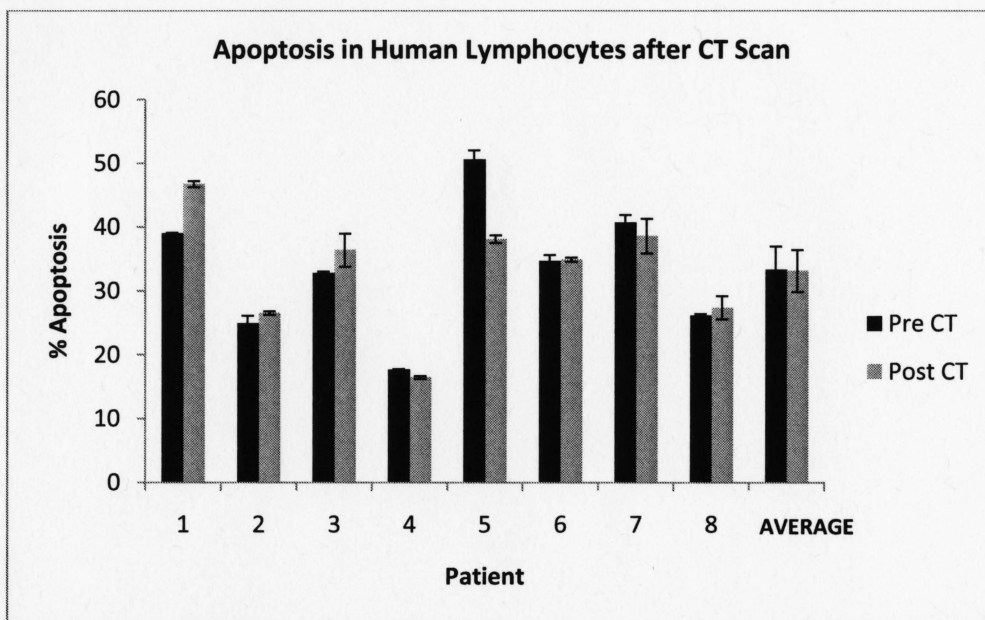


**Figure 3.1: Percent apoptosis in human lymphocytes following CT scan. Error bars for each patient represent standard error in 3 flow trials**

Following exposure *in vitro* of lymphocytes in supplemented media to 8 Gy  $\gamma$  rays resulted in dramatic increase in apoptosis for all patients by at least 28% (Figure 3.2). The average increase in apoptosis was ~43%. Inter-individual variation in radiation-induced apoptotic responses was observed before and after the CT scan, as well as before and after 8 Gy. Table C-3 in outlines percent differences in all patients after 8 Gy.

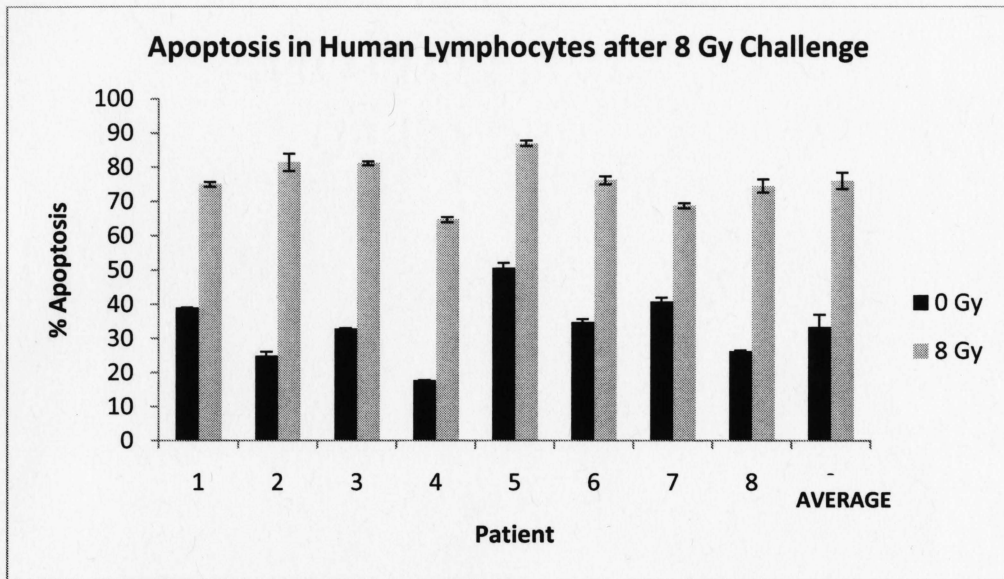


Figure 3.2: Percent apoptosis in human lymphocytes following irradiation at 0 and 8 Gy

Table 3.1: Apoptosis measured in human peripheral blood lymphocytes isolated from blood taken before and after a CT scan with 0 and 8 Gy gamma in vitro challenge doses

Patient #	0 Gy Challenge - % Apoptosis		8 Gy Challenge - % Apoptosis	
	Pre CT	Post CT	Pre CT	Post CT
1	39.00 ± 0.14	46.77 ± 0.47	75.06 ± 0.72	76.02 ± 0.09
2	24.90 ± 1.22	26.54 ± 0.26	81.47 ± 2.51	82.62
3	32.78 ± 0.25	36.39 ± 2.61	81.18 ± 0.52	77.44 ± 0.31
4	17.66 ± 0.15	16.48 ± 0.22	64.73 ± 0.72	67.17 ± 2.45
5	50.62 ± 1.46	38.11 ± 0.60	86.99 ± 0.79	77.39 ± 0.56
6	34.67 ± 0.97	34.91 ± 0.34	76.17 ± 1.15	75.54 ± 0.42
7	40.68 ± 1.25	38.61 ± 2.73	68.73 ± 0.75	66.38 ± 0.42
8	26.14 ± 0.30	27.39 ± 1.82	74.56 ± 1.91	74.98 ± 1.85
<b>AVERAGE</b>	<b>33.31 ± 3.67</b>	<b>33.15 ± 3.30</b>	<b>76.11 ± 2.37</b>	<b>74.57 ± 1.79</b>

*Adaptive Response was in observed for apoptosis in less than half of patient samples*

To detect the induction of an adaptive response, lymphocytes from blood collected before and after the CT scan were irradiated with 8 Gy as a challenge dose and

apoptosis was quantified. Results from flow cytometry show that in 3/8 patients, post-CT lymphocytes exhibited a significant decrease in apoptotic sensitivity following the large dose (Figure 3.3). Only one other patient showed lowered apoptosis but it was not significant. The remaining patients showed either a slight increase or stayed relatively the same. The average of all 8 patients showed a decrease of only 2 percent.

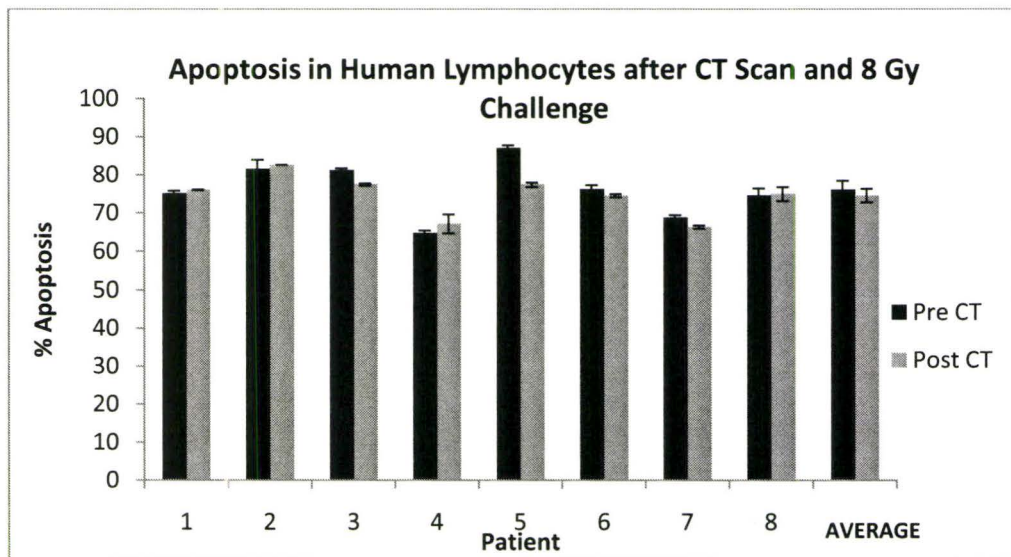


**Figure 3.3: Percent apoptosis in human lymphocytes following CT scan and 8 Gy in vitro challenge dose**

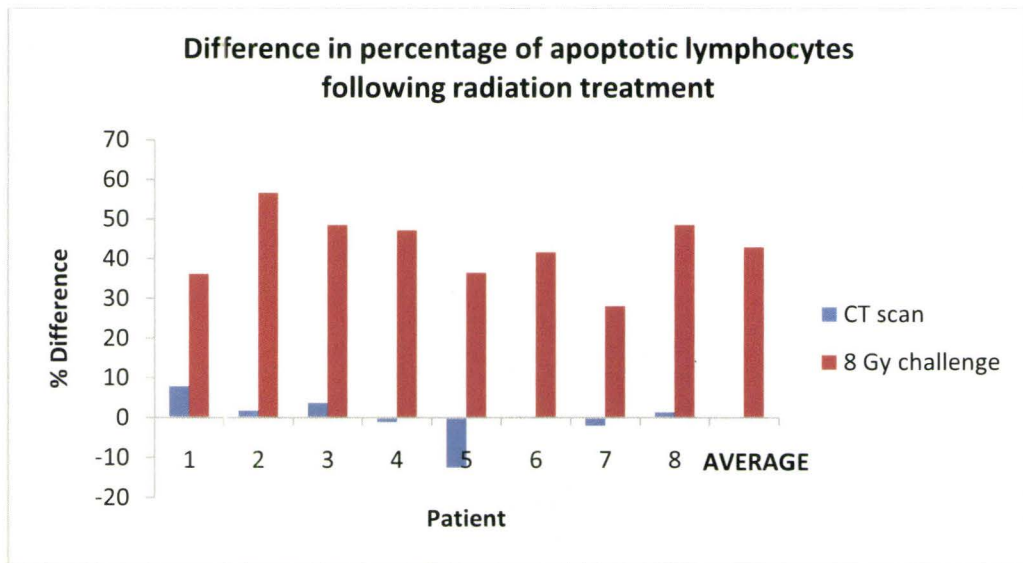


**Figure 3.4:** An overview of the percent differences in apoptosis in lymphocytes of all 8 patients before and after CT (blue) and before and after 8 Gy *in vitro* (red)

Figure 3.4 shows that there was no pattern seen amongst patients in radiation-induced apoptosis. For some individuals, a large increase in cell death following a CT scan did not show the same effect in response to a larger dose of 8 Gy. Patients 5 and 7, however, did show both a decrease in apoptosis following the CT as well as a weak cell death effect following 8 Gy. Overall these results confirm that inter-patient variation can be seen at high and low doses as well as following both *in vivo* and *in vitro* exposures.

### 3.2 DNA DOUBLE STRAND BREAKS

The mean fluorescence intensity of the  $\gamma$ -H2AX antibody measuring levels of H2AX phosphorylation was quantified before and after the CT scan as well as at a 0 and 8 Gy *in vitro* challenge dose. There was no observed difference before and after CT (Figure 3.5) but following 8 Gy there was a dramatic increase in H2AX phosphorylation



(Figure 3.6). This dose was able to elevate lethality in lymphocytes of every patient by a factor of at least 12. The error bars in both histograms represent standard error in the duplicate trials for each patient and treatment.

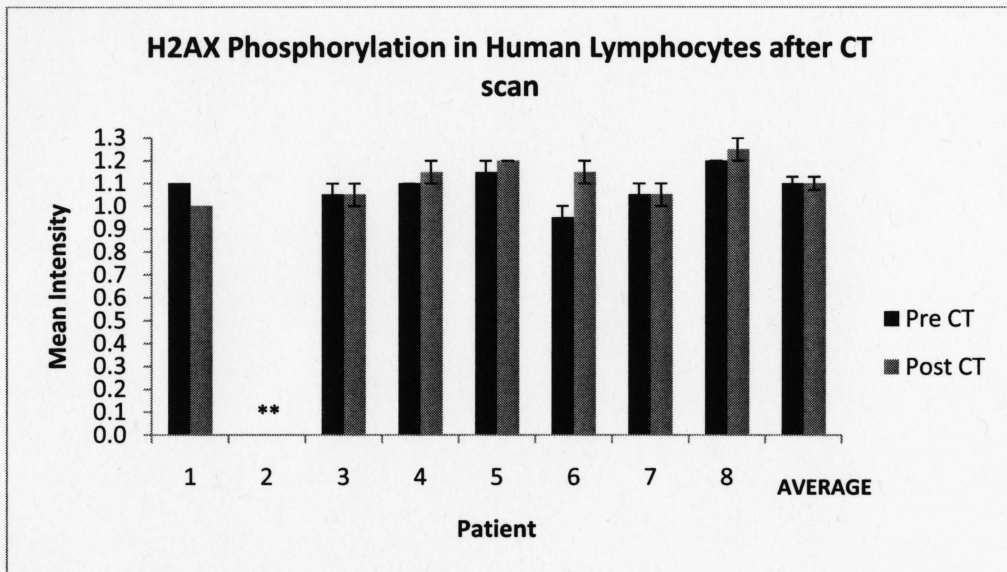


**Figure 3.5: Gamma H2AX phosphorylation in human lymphocytes as measured by fluorescence intensity following CT scan (\*\*Data not available)**



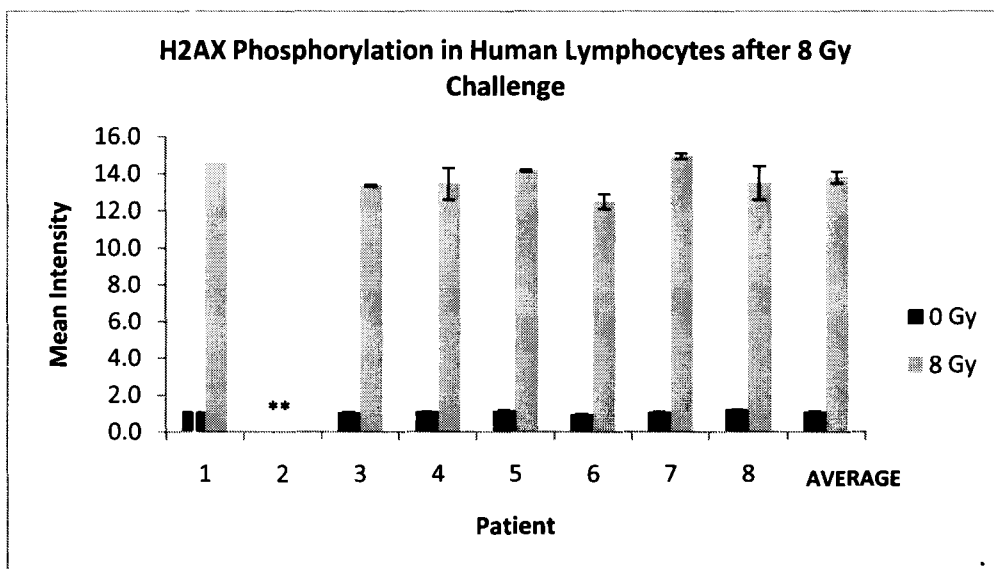


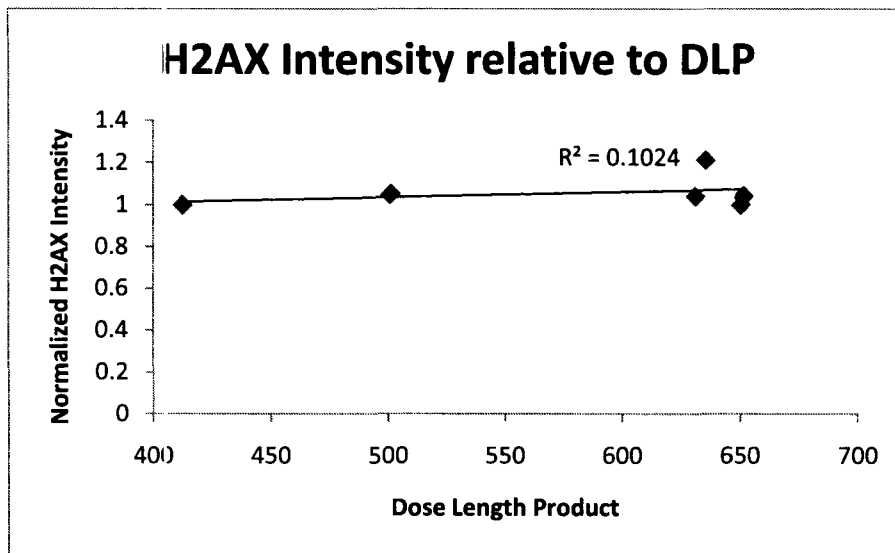
Figure 3.6: Gamma H2AX phosphorylation in human lymphocytes as measured by fluorescence intensity following 8 Gy *in vitro* challenge dose (\*\*Data not available)

Table 3.2: Levels of phosphorylated histone H2AX as measured by mean fluorescence intensity in human peripheral blood lymphocytes before and after a CT scan with 0 and 8 Gy gamma *in vitro* challenge doses\*

Patient #	0 Gy Challenge		8 Gy Challenge	
	Pre CT	Post CT	Pre CT	Post CT
1	1.1	1.0	14.6	13.8
2	no data	no data	no data	no data
3	1.1 ± 0.05	1.1 ± 0.05	13.4 ± 0.05	13.5
4	1.1	1.2 ± 0.05	13.5 ± 0.85	13.3 ± 0.25
5	1.2 ± 0.05	1.2	14.2 ± 0.05	12.5 ± 0.20
6	1.0 ± 0.05	1.2 ± 0.05	12.5 ± 0.40	13.0
7	1.1 ± 0.05	1.1 ± 0.05	15.0 ± 0.15	15.6 ± 0.75
8	1.20	1.3 ± 0.05	13.5 ± 0.90	13.3 ± 0.30
<b>AVERAGE</b>	<b>1.1 ± 0.03</b>	<b>1.1 ± 0.03</b>	<b>13.8 ± 0.32</b>	<b>13.6 ± 0.37</b>

\*Those values with no standard error indicate that both trials yielded the same mean intensity value

According to Figure 3.7, there was no correlation present between H2AX phosphorylation and the dose length product (DLP) of the CT scan. This suggests that minor differences observed in the induction of DSBs are not due to differences in dose.



**Figure 3.7: Graph showing relationship between level of H2AX phosphorylation and DLP values for pelvic CT. For patients who were scanned multiple times, results were obtained for the first scan only**

To determine whether the dose from the CT scan was able to modify the level of DSBs after 8 Gy, H2AX intensity was compared in pre and post CT lymphocytes. According to Figure 3.8, post-CT lymphocyte samples from only one patient showed a significant decrease in DNA damage after the 8 Gy challenge dose. This suggests that the adaptive response is possible but may vary depending on radiosensitivity. Level of

phosphorylated  $\gamma$ -H2AX formation in the remaining patients either increased slightly or decreased slightly or stayed about the same.

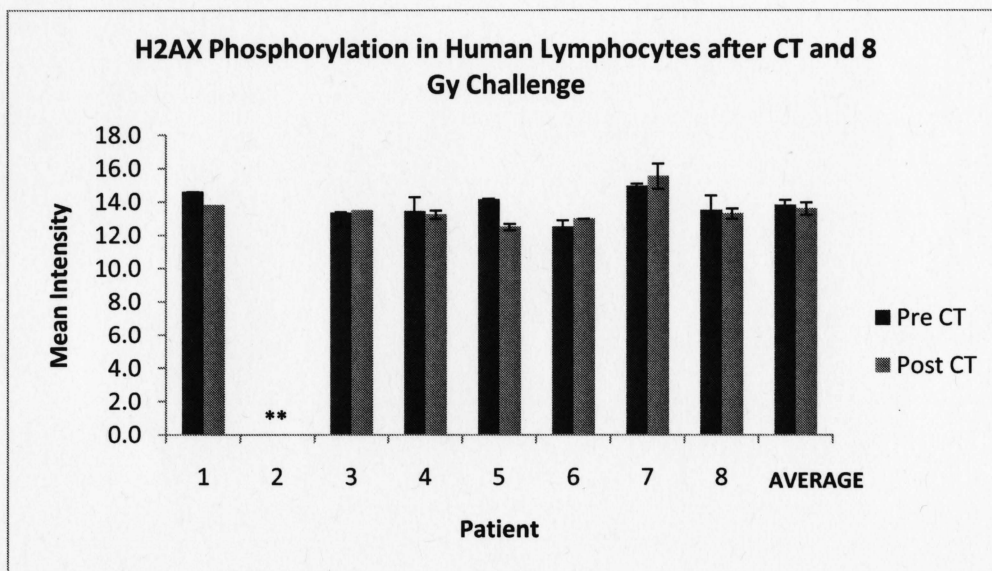
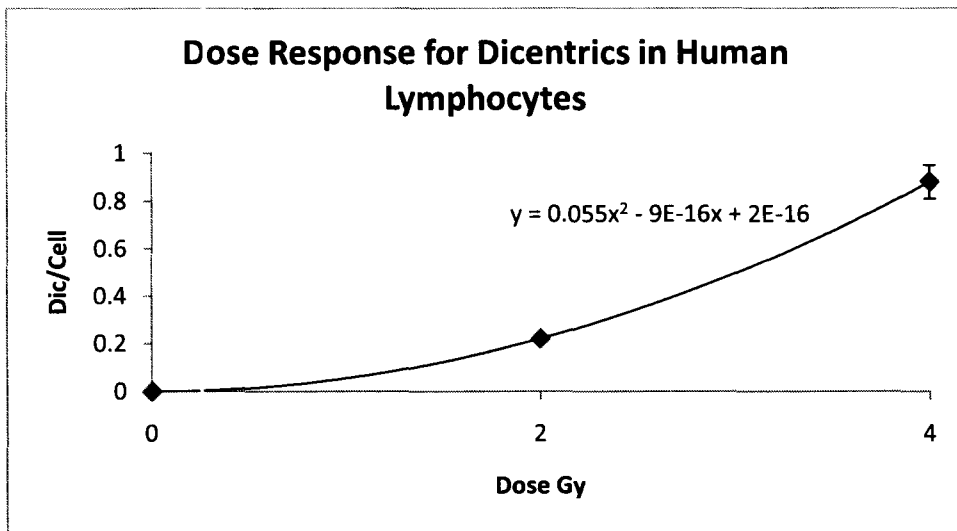


Figure 3.8: Gamma H2AX phosphorylation in human lymphocytes as measured by fluorescence intensity following CT scan and 8 Gy in vitro challenge dose (\* p-value<0.05 \*\*Data not available)

### 3.3 CHROMOSOME INSTABILITY

#### 3.3.1 Dose Response in Healthy Individuals

Blood collected from three healthy volunteers was irradiated at 0, 2, and 4 Gy. Samples were fixed and dropped manually on slides in preparation for microscope scoring. Two hundred metaphases were observed for each dose and a dose curve was generated (Figure 3.9). The relationship between dicentric frequency and dose was linear quadratic.



**Figure 3.9: Dose-response for curve for dicentric at 0, 2, and 4 Gy gamma rays. Each point represents the average of three volunteers (two male, one female).**

### 3.3.2 Frequency of Aberrations in patients following CT scan and 3 Gy

Whole blood collected before and after the CT was fixed and good quality slides yielding a high percentage of M1 metaphases were used to score dicentric for each patient and treatment (pre and post CT, pre CT + 3 Gy and post CT + 3 Gy). No significant effect on the frequency of chromosome aberrations was detected following CT ( $p=0.1$ ). However, 4/8 patients showed slight elevation above the natural background frequency with ~1-2 dicentric scored in 150-200 cells.

**Table 3.3: Frequency of dicentrics per cell for each patient with average values for each treatment**

Patient	Treatment			
	Pre CT	Post CT	Pre CT + 3 Gy	Post CT + 3 Gy
1	0.005	0.005	0.365	0.167
2	0	0	0.523	0.432
3	0.005	0	0.528	0.525
4	0	0.005	0.382	0.451
5	0	0.007	0.510	0.530
6	0	0.013	0.640	0.470
7	0	0.007	0.588	0.536
8	0	0	0.510	0.480
<b>Average</b>	<b>0.001</b>	<b>0.005</b>	<b>0.506</b>	<b>0.449</b>

Figure 3.92 shows that after irradiation with 3 Gy, there was a dramatic increase in the frequency of dicentrics/cell with a large degree of variation across patients. Some metaphases showed up to 4 dicentrics and there was also presence of tricentrics (chromosomes having 3 centromeres) in a small proportion of cells (Figure 3.91). Only cells with 46 chromosomes and found within the first division were scored to eliminate offsetting the frequency of aberrations. Interestingly, some patients also showed a greater reduction in mitotic index than others after 3 Gy, which is further evidence for variation in radiation sensitivity. Full data on number of metaphases scored and number of dicentrics identified can be found in Table C-4.

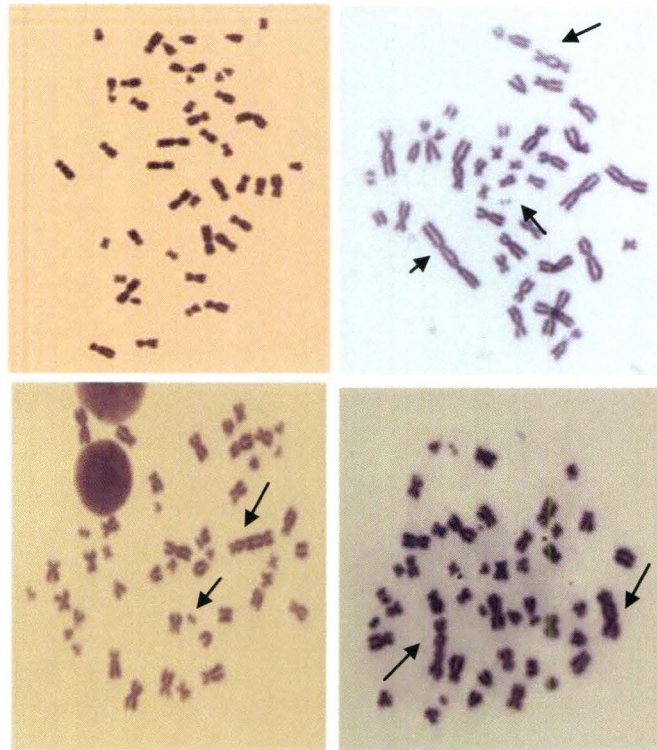


**Figure 3.91: Microscopy images of metaphase spreads. Top L) Normal met with 46 chromosomes and no apparent aberrations present. Top R) Taken from a 3 Gy sample, note the presence multiple dicentrics with corresponding acentric fragments within a single metaphase (arrow) Bottom L) Also from 3 Gy. Note presence of tricentrics (arrow). Bottom R) Also from 3 Gy with dicentrics and tricentrics present**



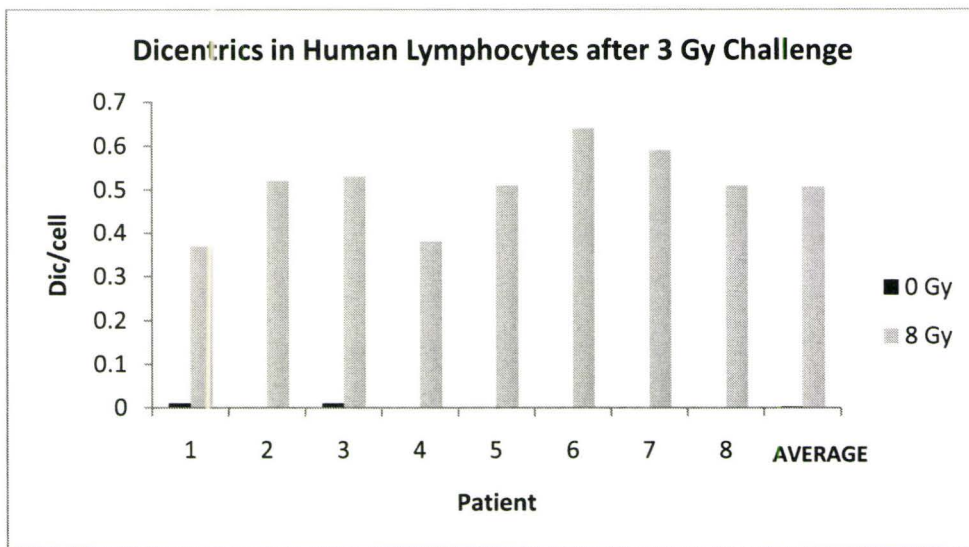


Figure 3.92: Frequency of dicentric in whole blood following 3 Gy *in vitro*

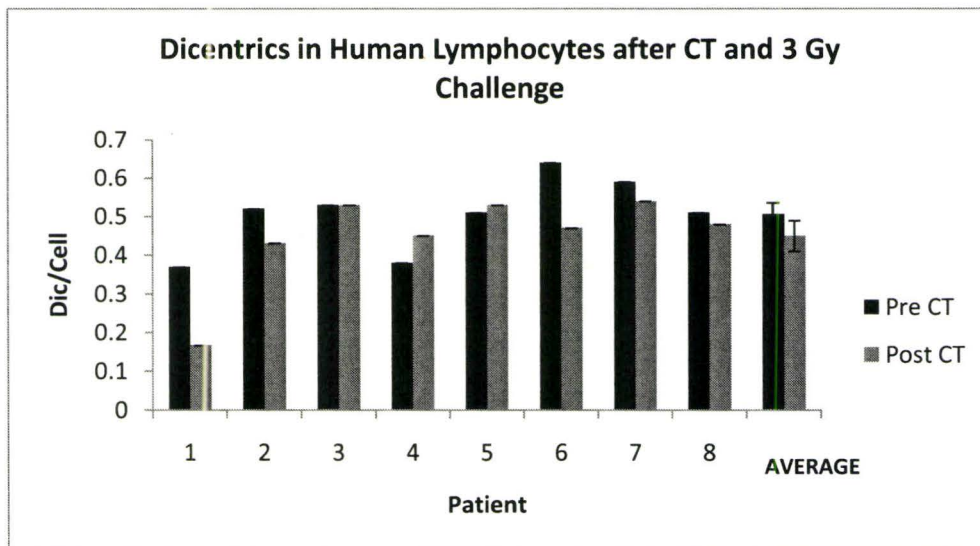


Figure 3.93: Frequency of dicentric in human lymphocytes following CT scan and 3 Gy *in vitro* challenge dose (p-value=0.3)

Figure 3.93 shows that the adaptive response may have occurred in the cells of some patients (1, 2, 6, 7, and 8) following the CT priming dose and subsequent 3 Gy challenge dose. Other patients, however, either showed the same frequency (patient 3) or

an increase (4 and 5). Overall there was an average decrease in dicentric frequency in the CT + 3Gy samples (grey bars) vs. 3 Gy only (no CT, black bars) but it did not appear to be significant ( $p=0.3$ )

#### 4. DISCUSSION

##### *Individual differences in radiation induced biological effects and radiosensitivity*

Inter-individual variation in radiosensitivity is a genetically controlled biological phenomenon whose investigation spans decades. The differences in cellular responses to radiation present a challenge to international limits enabled by LNT models of mutagenesis and carcinogenesis [55]. These policies are based on the assumption that people respond to radiation the same and thus succumb to the same increased risk for cancer upon exposure [30]. It would be very difficult to tailor dose limits to accommodate all degrees of radiosensitivities amongst individuals. However, understanding the biological mechanisms that give rise to such variation and the degree to which a specific population of interest varies is beneficial for medicine, biodosimetry, and risk assessment [30].

A cell's DNA controls all metabolic and physiological processes within a cell, but is also a major target for radiation-induced damage. Given this it is expected that, upon exposure to both high and low-LET radiation, biological changes resulting from DNA damage will occur. Endpoints such as apoptosis, DNA DSBs, and chromosome aberrations, mutation frequency, clonogenic survival [52], activation of checkpoint arrest, and micronuclei [53] are all sensitive to radiation and have also shown some level of inter-individual variation. This disparity can be further exaggerated by differences in age, lifestyle, and cellular microenvironment.

The main purposes for this study were not only to examine the biological effects of CT scans, but also the degree to which individuals vary in their responses to radiation. A series of similar experiments were completed in this lab but with only 6 patients. The results of that study were limited by the small sample size and thus we have added additional patients to further strengthen the evidence previous seen.

Flow cytometry was used to determine the degree of programmed cell death and DNA DSB induction in lymphocytes. Percent apoptosis is the proportion of gated mononuclear cells (determined to be lymphocytes based on forward and side scatter) that are positive for Annexin V, which binds to externalized phosphatidylserine on the outer membrane during early apoptosis. Cells proceeding into the late apoptotic-early necrotic phase were excluded by enumerating cells which were Annexin<sup>+</sup> and negative for the viability dye 7AAD.

The results these experiments show that, after irradiation of lymphocytes *in vitro* with 8 Gy, both levels of apoptosis and phosphorylation of histone H2AX increased dramatically in all 8 patients (Tables 3.2 and 3.6). Patients 1, 5 and 7 displayed a relatively larger increase in H2AX intensity after 8 Gy, translating to greater genomic damage. These three patients however experienced a relatively lower radiation-induced increase in apoptosis after 8 Gy (Note the red bars in Figure 3.4). Although more phosphorylation of H2AX is interpreted as enhanced DSB damage, it can also be seen as increased foci formation or repair activation. Phosphorylation of the histone protein H2AX is a critical step in the DNA repair process, downstream of damage detection by

sensor proteins and ATM autophosphorylation. The formation of H2AX foci is required for further deconstruction of the chromatin and subsequent recruitment of repair factors such as 53BP1 and BRCA1/2 [34, 54]. Lymphocytes from these patients may have undergone repair in an attempt to reconstitute the radiation-induced lesions before resorting to the apoptotic pathway. This split decision between death and survival is dependent on the speed and accuracy of mechanisms whereby a cell can monitor genomic integrity and repair IR-induced assault as it occurs [54]. Whether or not this may be the case, results from this part of the study are another example of variation in radiation responses for both apoptosis and H2AX phosphorylation and prompts further investigation on the mutual exclusivity of these two processes within a cell.

Inter-individual variation can also be seen in spontaneous levels of apoptosis alone. The black bars in Figure 3.1 show that after a 44 hour incubation period with supplemented RPMI, spontaneous levels of programmed cell death in lymphocytes ranged anywhere from 17-50% (Table C-3, Part A). The average percentage of apoptotic lymphocytes for all patients was  $33.31 \pm 3.67\%$ , a value almost 10 percent higher than that obtained in the previous experiment amongst the 6 patients. The percent frequency of apoptotic lymphocytes following 8 Gy was also significantly higher this time (the highest recorded value in the first experiment was 40%, whereas in this case the average percent apoptosis was  $76.11 \pm 2.37\%$ ). There are several reasons why this may be the case. Previously, the average elapsed time from blood collection to processing was ~2 hours, an hour less than this time. Although blood was transported at the same temperature and in heparinized tubes, the difference in time can lead to intracellular perturbations that can

alter the kinetics of spontaneous lymphocyte apoptosis. Additionally, in the first experiment the PS-binding Annexin V/7AAD flow kit was used in conjunction with an anti CD45-antibody. CD45 is found on the surface of leukocytes, with the highest fluorescence expression in both T and B lymphocytes. Identification of this protein has vital implications in monitoring disease progression in HIV<sup>+</sup> patients [57, 58] who experience a steady depletion in their CD4<sup>+</sup> helper T cells. The use of this probe during flow analysis can help identify with high specificity the lymphocyte population within a heterogeneous monocyte culture. Although the FS and SS patterns are tight and easily identified for lymphocytes, confirming that the gated population from which fluorescence data is extracted are indeed T and B cells will yield more accurate results. Other factors such as differences in disease progression, age, medical history and even changes in CT scan protocol may have contributed to the difference observed between results from this cohort and the previous one. Dose Length Product (DLP) values in both studies were similar, which excludes dose from the CT as a possible factor in differences. Those patients who underwent multiple CTs were treated the same, with one blood collection taking place before and after the first scan only.

Aside from genetic predisposition, there are other possible reasons for the observed patient differences in intrinsic susceptibility of lymphocytes to radiation-induced apoptosis. A study published in 2003 by Schmitz *et al.* [59] looked at radiosensitivity of lymphocyte subpopulations irradiated *in vitro*. Annexin V-labeled CD4<sup>+</sup> helper T cells, CD8<sup>+</sup> killer T cells, and B cells were evaluated using flow cytometry, which showed that there are differences in both spontaneous and radiation-



induced apoptosis amongst these subsets, with T cells showing greater radioresistance than B cells. This divergence in apoptotic sensitivity may explain patient differences observed in this and other studies. Monocyte fractions isolated on Histopaque are heterogeneous populations containing variable ratios of CD4<sup>+</sup>, CD8<sup>+</sup>, and B cells. The level of apoptosis measured in these samples will therefore depend on the proportion of each lymphocyte subpopulation.

The notion that DNA damage repair processes and apoptotic responses vary among individuals has further importance with regards to radiotherapy, which comprises a large portion of cancer treatment regimens. A percentage of patients that undergo external beam radiation therapy (EBRT) will experience normal tissue toxicity years after treatment [30]. Using current knowledge on inter-individual variation in tissue sensitivity to radiation, research on a rapid, functional *in vitro* assay that can help physicians identify patients who may experience an adverse reaction to treatment becomes of increasing importance [30, 52, 60-62]. A study published in 2009 by Schnarr *et al* [21] observed apoptosis in lymphocytes from prostate cancer patients who experienced increased late toxicity using flow analysis Annexin V-FITC labeled cells. Results from this predictive assay showed that patients succumbing to late toxicity had an apoptotic response at or below the mean for all patients undergoing radiotherapy. This confirmed the hypothesis that low levels of apoptosis may confer radiosensitivity and thus increase the likelihood of a patient experiencing unfavorable symptoms due to the reduced ability of cells to recognize and eliminate damage [21, 47].

Other studies have attempted to predict intrinsic levels of radiosensitivity using other biological markers such as the frequency of chromosome aberrations [61], and rate of DSB induction and repair following IR exposure *in vitro* and *in vivo* [37, 60]. Following fibroblast analysis of a patient who experienced severe side effects of radiation therapy, Löbrich *et al* were able to identify a significantly higher excess of H2AX foci up to 24 hours after a CT scan in comparison to the other patients, which suggests that this person may have repair deficiencies resulting in negative symptoms. There is enough convincing evidence that following IR, the slow loss of H2AX foci observed translates to a slow rejoining of DSBs [37, 60]. Another question stemming from this is whether this ‘slow’ response means greater radiosensitivity. Although  $\gamma$ -H2AX holds promise as a biological indicator of tissue resistance as it is an endpoint that can be quantified at very low doses, there are still challenges assigned to this assay as repair *fidelity* may be of greater importance than speed of repair, and that is much more difficult to measure [60].

When establishing an appropriate method for predicting radiosensitivity in patients in order to enhance patient care following radiation therapy, reproducibility is most important. Potential biological markers should ideally be radiation-specific and their detection requires high sensitivity. For apoptosis, intraindividual variation may depend on factors such as infection, fatigue, exercise, or drug and alcohol consumption [21]. Undertaking several experiments with each patient after a specified amount of time in between can help researchers better recognize patterns in lymphocyte apoptosis and other endpoints to determine the degree of radiosensitivity.

Inter-individual differences were observed not only for apoptosis and DNA DSBs, but also for chromosome aberrations. After irradiation with 3 Gy, whole blood collected from volunteers for the dicentric assay was fixed and scored using microscopy. According to Figure 3.92, the frequency of chromosomes possessing two centromeres as a result of replication of misrepaired DNA increased significantly after irradiation but also varied amongst individuals. Patient 6 demonstrated a significant increase in frequency of dicentrics, starting from none scored to more than half of cells possessing dicentric chromosomes, while the frequency observed in patients 1 and 4 increased up to just 30% after 3 Gy. Interestingly, two of the eight patients scored 1 dicentric in ~200 cells analyzed (frequency = 0.005) which is higher than the documented natural background rate for dicentrics in observed human populations (background rate is ~1 in 2000, 0.0005). Although dicentrics are a lethal aberration, some cells are still able to maintain the misrepaired DNA damage in the nucleus, formed by increased exposure to natural or man-made sources of radiation or by other genotoxic agents. A low spontaneous level of dicentrics was also present in the first study, however after a 3 Gy challenge dose, the frequency increased to those ~0.1-0.3 dic/cell, which is almost 50% less than what was seen this time.

Fluorescence plus giemsa revealed a small but insignificant increase in dicentric frequency observed before and after the CT within this cohort (p-value=0.1). Stephan *et al* [8] reported an enhanced yield of aberrations in pediatric patients aged 0.4-15 years old following CT, with emphases on the younger group of children whose increase was significant. Although this might be expected as younger children are deemed more

radiosensitive, evidence from our study show no age-effect for dicentrics, at least from a high dose.

To demonstrate the dose-dependent nature of dicentric formation, a dose response curve was generated using blood from three, young healthy volunteers. Samples were irradiated with 0, 2 and 4 Gy, and a linear quadratic relationship was discovered (Figure 3.9). Interestingly, the dicentric frequency value obtained for 3 Gy using this curve (0.49 dic/cell) was very similar to the average value scored for all 8 patients (0.51 dic/cell). This suggests that, as stated, dicentric frequency may not be dependent on age, although more volunteers should be included to strengthen the statistical power of this claim. A recent publication from Health Canada and the Canadian Cytogenetic Emergency Network (CEN) reported a dicentric frequency of ~0.75 from a 3 Gy *in vitro* exposure to Cs<sup>137</sup>  $\gamma$ -rays. This value is slightly higher but includes the number of rings as well [63].

It is ideal to score between 500-1000 metaphases in the case of low doses. Doses greater than 1 Gy produce more breaks and thus ~100 metaphases should provide an accurate estimation of dose or damage produced by a known dose [40]. For this study, ~150-200 metaphases were analyzed for each treatment – before and after CT, and before and after CT + 3 Gy *in vitro*  $\gamma$ -rays. If additional cells were scored perhaps the frequency would be altered slightly. The previous study using 6 patients only scored 50 metaphases which may be the reason for the observed differences in frequency.

In the future, adding to current evidence using alternative cytogenetic techniques may be useful in determining the level of radiation-induced chromosome aberrations. Stable translocations, for example have been validated as a useful biomarker and has been looked at in this lab using mice and human lymphocytes as well as cells within the bone marrow. Its use in dosimetry and implications in radiocarcinogenesis, however, is limited due to a higher background frequency (up to 10/1000 cells) than dicentrics and reported significant inter-individual variation above the age of 40 [38]. Methods such as SKY are also costly and more time consuming than conventional Giemsa staining (although the latter cannot detect the presence of balanced translocations). M'kacher *et al* [64] measured the aberration frequency in lymphocytes of 10 patients before after a CT scan using Fluorescence in situ Hybridization (FISH). They were not able to detect a significant increase in aberration frequency, but did measure an increase in fragments when using the Premature Chromosome Condensation (PCC) assay.

### ***Intrinsic cellular responses to radiation for in vivo and in vitro exposures***

There is ongoing debate and conflicting evidence regarding the differential responses of cells to low and high doses of radiation. The LNT model for radiation-associated carcinogenic risk is based mainly on data from populations exposed to high doses such as the survivors of the atomic bomb in Hiroshima and Nagasaki. Estimates drawn for this back extrapolation form the basis of radiation protection standards. Epidemiological data on low doses, however, is limited and lacks statistical evidence to



accurately estimate cancer risk from low dose and dose-rate exposures [65]. In 2005, The Joint Report of the French National Academies of Science and of Medicine published the “French Report” outlining data on risks associated with low dose ionizing radiation. The document maintained that there were no epidemiological studies showing an increase in cancer incidence for doses less than 100mSv [66]. This adds importance to animal and cellular experiments which have become increasingly important in the elucidation of radiobiological effects at lower doses and dose-rates.

When considering a linear, non-threshold model one of the underlying assumptions is that irradiation of a cell will lead to an increasing probability of mutations, error-free repair, misrepair, or apoptosis proportional to increasing dose [52]. The data from this study demonstrate that that is not the case. Rather, lymphocytes from the 8 patients show a high degree of inter individual variation in: spontaneous levels of apoptosis, apoptosis induced by a single CT scan, apoptosis induced by 8 Gy and apoptosis changes during the adaptive response. While some patients display a dramatic increase in apoptosis following either the CT scan or *in vitro* challenge dose, others show a decrease in cell death or stay relatively the same. The next question would be whether radio-induced apoptotic responses can predict an individual’s radiosensitivity or robustness of repair and antioxidant mechanisms.

Lymphocytes from Patient 1 showed a significant increase in apoptosis following CT scan but a weak apoptotic response following 8 Gy exposure *in vitro*. This is evidence that cells respond to low and high doses of radiation differently, and that experiments



which assay apoptosis at low levels may not be able to predict cellular reactions to high doses. The 8% increase in apoptosis seen in this patient following CT may be an indication of low-dose hypersensitivity more so than conferred radioresistance. This may also be due inactivated repair mechanisms at low dose exposures. Some evidence based on biomarkers for DNA damage signaling pathways such as ATM, ATR and H2AX phosphorylation show that although repair takes place at higher doses of radiation, they appear to be absent at lower dose and dose rates [37, 68]. If the dose is too low for this patient's lymphocytes to undergo sufficient repair it may lead to an elevation in cell death [55]. Whatever the case, apoptosis is regarded as a kinetically slow, protein-synthesis dependent process [27], which can help to explain the different responses observed after 8 Gy in comparison to the CT scan. Perhaps this hypersensitivity promoted the upregulation of repair and antioxidant genes, resulting in lowered cell death than what was seen in other patients after high dose IR. In the context of predicting tissue radiosensitivity in clinical practice, one could argue that the lowered apoptotic response for this patient after 8 Gy means he is radiosensitive due to the inherent inability to eliminate damaged cells. However, a small increase in apoptosis could also be interpreted as an increase in repair, cell survival, although it remains unclear whether it is an error-free restitution of genomic integrity.

Low-dose hypersensitivity is defined as an increase in cell lethality following low doses of radiation with greater resistance at higher doses [70]. The excessive sensitivity alters the cell-survival curve and thus cannot be predicted by back extrapolating using data from high doses [71]. Although this hypersensitive response is clearly observed in

the first patient, the outcome does not seem to apply to the other patients sampled in this study, particularly patients 5 and 7. Cytometric analysis of lymphocytes from these patients showed a decrease in apoptosis following a CT scan, but also showed a relatively low induction of apoptosis following 8 Gy. Although they appear to be slightly more resistant to radiation induced lethality at high doses, they also exhibit resistance to cell death at low doses. It is possible that individuals such as these patients possess robust radioprotective pathways that maintain cell survival or, alternatively, lack the ability to kill cells harboring damage from any dose.

In order to fully test the level of radiosensitivity of patients, it would be ideal to monitor them throughout the course of their radiation therapy. Observing signs of cellular toxicity or sampling lymphocytes at different time-points can shed light on whether the increase or decrease in apoptosis observed early on match any clinical symptoms or cellular changes *in vivo*. It may also be possible to observe clonogenic capacity by culturing lymphoblastoid cell lines from the peripheral blood of each patient, which was achieved by Leong *et al.* [52] in their attempt to observe radiosensitivity in lymphocytes of patients who experienced severe toxicity from treatment.

A more interesting result from the apoptosis experiment was that, despite a significant decrease in apoptosis following the CT scan as well as a relatively lower cell death response after IR with 8 Gy, patient 5 showed the highest level of spontaneous apoptosis. About 50 percent of the gated unirradiated lymphocytes for this patient were Annexin V<sup>+</sup>, meaning nearly half of the cells were apoptotic in the absence of any

treatment. Patient 7, which also showed a weak apoptotic response to both the CT and 8 Gy, also showed high levels of spontaneous apoptosis, with 40% of lymphocytes dying without any IR. This present additional difficulty in using apoptosis, at least naturally occurring apoptosis, to determine radiation responses, either to high doses *in vitro* or in the clinical setting. This also, once again, challenges the LNT model for carcinogenic risk which assumes that, at doses below 100 mGy, individuals will exhibit the same rates of mutation, DNA damage repair, and apoptosis resulting in a defined value of increased risk for cancer.

Patient 2, 3 and 8 cells showed the largest increase in apoptosis following an 8 Gy challenge. In contrast to was seen with patients 5 and 7, samples collected from these men after their CT scan showed slight elevation in apoptosis (~1.5-4% increase), but it was not significant. Again this illustrated patient differences in responses to radiation, with even greater variation in the responses to high vs. low doses. For patient 1, the observed hypersensitivity did not confer an elevated response following 8 Gy. Alternative, for patients 2, 3, and 6, where apoptosis still increased but only slightly, there was a dramatic elevation in apoptosis following the challenge dose (~48-57 % increase). If apoptosis can be used as a measure of sensitivity, then these patients in particular may be considered radioresistant. Based on this notion it can be assumed that if they decide to pursue radiotherapy they will be less likely to succumb to normal tissue toxicity due their ability to eliminate cells containing radiation damage [47]. The same theory applies to normal cells that have been exposed to mutagenic agents. Failure to remove cells with genetic damage can contribute to the development of cancer [73].

However we go back to the question of whether these patients may also have defective repair mechanisms at high doses, leading to a 50 percent increase in apoptotic lymphocytes. According to Graph, patients 3 and 8 show similar levels of H2AX phosphorylation following 8 Gy, in comparison to patients 5 and 7 which show slightly higher levels of phosphorylation which may support this speculation that the increase in H2AX intensity may be a signal for increased repair, resulting in a relatively lower level of apoptosis for patients 5 and 7.

Patient 4, 5, and 7 cells showed a decrease in apoptotic levels following the CT scan. The decrease was especially significant in patient 5, who interestingly had the highest level of spontaneous apoptosis. This could mean that higher spontaneous levels of cell death may dictate increased radiosensitivity as shown here with a very pronounced decrease in apoptosis following the CT scan. This patient may be more likely to experience negative side effects from cancer therapy due to their inability to remove damaged cells, although this seems inconsistent with the fact that, under unirradiated conditions, apoptosis levels are high. Again, this could be the result of the relative proportions of lymphocyte subpopulations in the sample. It could be that more B cells were present, altering values for positive Annexin V binding.

Overall these differences verify that, at both low and high doses of ionizing radiation, cells respond differently through genetically controlled mechanisms that. Some patients showed a considerable increase or decrease in apoptosis following either a CT scan or 8 Gy *in vitro* challenge dose, while other patients showed less change or no

change at all. Whatever the case, these changes are most likely due to radiation exposure. To further demonstrate this, a sham CT experiment was conducted in a male volunteer whose age fell in between the range of the 8 patients. According to Figure C-1 the level of apoptosis stayed the same before and after the CT and was very similar to the average frequency of apoptosis measured in the cohort as well as the average spontaneous level of apoptosis. Although only one control was conducted, the results demonstrate that the changes observed in the lymphocytes are more likely due to radiation than noise because of the more prominent differences seen in comparison to the sham CT control. Previous studies have argued that the spontaneous frequency of apoptosis in unirradiated cells is a vital determinant of apoptotic responses following radiation [23]. However in this study the variation observed amongst patients and the inability to find a relationship between background apoptosis and apoptosis induced by both a small and large dose disputes this notion. Additional implications of this work are the effect of age on radiation-induced apoptosis, particular the correlation between age and assays such as the Annexin-7AAD and other similar flow-based techniques. Schnarr *et al* discovered a weak positive linear relationship between age and percent apoptosis as determined by Annexin binding. The results also that above 60 years of age, the number of apoptotic lymphocytes is much more dispersed and ranged anywhere from 0% up to 30% [30]. Perhaps in the case of this study age may have been a factor in variation observed, and so further investigation into that area is required.

***Double strand breaks in lymphocytes following a CT scan***

Early techniques developed to assay the induction of DNA DSBs were able to identify the histone H2AX as a target protein whose phosphorylation is vital to repair following ionizing radiation [36]. Previous similar studies involving microscopy and pulse-field gel electrophoresis (PFGE) show that the amount of DNA DSBs induced by IR is in fact proportional to the level of phosphorylation of histone H2AX, validating  $\gamma$ -H2AX as a highly specific marker genotoxicity [37]. Some reviews, however, still argue that although it is accepted that a DSB break results in an H2AX focus, not all H2AX foci may necessarily be DSBs. There have been ways to overcome the challenges in assaying for H2AX as a measure of DSB induction, including the use of PI to determine those cells that are not cycling and therefore would not have elevated baseline H2AX levels cause by normal endogenous processes such as V(D)J recombination [11] and DNA replication. Although kinetics for  $\gamma$ -H2AX detection are normally optimized in each experiment, there is still ongoing work being done on rate of repair as determined by loss of H2AX foci over time. Complete repair requires full restoration of the chromatin structure which may be facilitated by the presence of  $\gamma$ -H2AX [34]. Therefore the detection of residual foci hours up to days following IR may translate to an ongoing repair process long after the damage had been attended to.

One of the central purposes of this study was to examine the induction of DNA DSBs in lymphocytes following a CT scan and *in vitro* irradiation with 8 Gy using flow cytometric analysis of  $\gamma$ -H2AX. Lymphocytes collected before the CT were irradiated at



the Taylor source, incubated at 37°C for half an hour and kept in 70% ethanol for one week, at which point samples were labeled with an anti H2AX antibody and analyzed based on fluorescence intensity. Following exposure with 8 Gy, levels of H2AX phosphorylation in lymphocytes increased up to 14 times validating its presence as an indicator of DSBs. Some patients showed slightly less DNA damage than others, which could be based on a number of factors including genetically controlled radiosensitivity, age, and lifestyle. Variation between individuals was not as large as what was observed for apoptosis following 8 Gy. Low levels of  $\gamma$ -H2AX were still detected in unirradiated lymphocytes, which may be due to the presence of ‘microfoci’ which have been observed in senescent cells and do not associate with repair factors [34].

H2AX phosphorylation, however, was absent at all in cells before and after the CT scan. This raises questions regarding: time allowance for repair, sensitivity of the H2AX flow assay at lower doses, and the possibility of repair evasion at low dose and dose-rates. From the time of initial blood collection to the arrival of samples at McMaster for processing approximately 3 hours had passed, with the second collection taking place ~1 hour after the first (patients needed time to prepare for the scan and walk to and from the blood lab). Similar with apoptosis, the induction and subsequent loss of H2AX foci following IR depends on the dose, irradiation conditions, radiation quality and the use of whole blood versus isolated lymphocytes [69]. Upon careful review of previous studies observing  $\gamma$ -H2AX induction in lymphocytes reveals different results as each of the aforementioned conditions are modified.

A recent publication by Beels *et al* [69] observed delayed repair in lymphocytes following *in vitro* irradiation with 5 and 200 mGy x-rays. After 24 hours, 40% of foci were still present in the whole blood, and 10% was still observed in isolated T lymphocytes. Values were slightly lower for Co<sup>60</sup>  $\gamma$ -rays, where almost half of the initial H2AX foci had disappeared 3 hours post treatment. Overall their data confirms speculation that at doses ~200 mGy, lymphocytes exhibit a repair half-life of about 3.5-4 hours which brings up the question of whether, in this CT study, there was too long of time lapse between the scan and processing of the blood at McMaster. It must be kept in mind, however, that in the above experiments irradiations were done *in vitro* and a more rapid repair response was observed for  $\gamma$ -rays, where in our case the lymphocytes were exposed *in vivo* to x-rays from the CT.

When looking at the rate of H2AX loss following 3-phase CT scans of the thorax and abdomen (DLP values from 150-1500 mGy cm), Löbrich *et al.* analyzed isolated lymphocyte samples at 30 and 60 mins post CT IR. They discovered a peak value for foci formation at 30 minutes and that at this time, the number of foci increased linearly with increasing DLP value for each patient. They argued that the high foci number at 30 mins coincides with the notion that DNA repair typically occurs between 30 to 60 min. This brings up additional concern for my study, which also detects *in vivo* DSB induction in lymphocytes following a pelvic CT. If there a possibility for repair within a 30-60 minute window post irradiation, then the value measured hours later in this case may not be a true indication of damage produced by the radiation. However, in the same CT study by Löbrich, they also looked at the *in vivo* kinetics of  $\gamma$ -H2AX foci loss and found that

phosphorylation of this histone was still apparent up 24 hours post IR when levels returned to baseline [37]. In addition to this, researchers also irradiated the lymphocytes *in vitro* with 5 mGy and observed 50% of foci remaining after 5 hours. They also performed an additional irradiation with 500 mGy, and observed a 90% loss of foci after 5 hours. The *in vitro* experiments show slower repair than what was seen *in vivo* following the CT scan, which may be a reflection of the differences caused by changes in irradiation settings. Regardless, both components of the study demonstrate the existence of a very low detection limit for DBSs assayed by phosphorylated H2AX, and that foci can still persist hours after irradiation, although this value declines with time making it difficult to determine how much damage was initially produced.

Both studies exemplify the degree to which the formation of  $\gamma$ -H2AX foci and subsequent loss over time post-IR vary based on changes in dose, irradiation conditions, and radiation quality. Further, differential H2AX responses in lymphocyte subsets appear to be minimal [20], which is not the case for apoptosis and may explain why more inter patient variation was observed in the latter.

What is more interesting is the observation that, upon exposure to low dose radiation, cells appear to evade the repair response. This may explain why no changes in  $\gamma$ -H2AX formation were seen following the CT scan in this study. Collis *et al* [67] reported a dramatic reduction in ATM phosphorylation in several human cell lines following exposure to a dose of ionizing radiation delivered at a low dose rate versus the same dose delivered at a high dose rate. Flow cytometric analysis also revealed lowered

levels of H2AX phosphorylation which re-affirms the role of  $\gamma$ -H2AX as a DNA damage repair signal downstream of ATM. This is evidence of an inactivated or abrogated repair response in cells following low-dose radiation in comparison to cells treated with a dose rate several orders of magnitude higher. This inactivation may have contributed to an observed increase in cell lethality. This ‘inverse dose rate’ effect was also demonstrated in human fibroblasts, and lead researchers to believe that the evasion of DNA damage sensing and repair activation may be done to avoid surviving at an increased risk of mutation. This response was seen again by Rothkamm and Löbrich who, after treatment of nondividing human fibroblasts with radiation as low as 1 mGy x-rays, discovered the presence of unrepaired DBSs by monitoring the persistence of foci which increased above background levels but did not subside until days after exposure [69].

Overall, the lack of a significant increase or decrease in H2AX phosphorylation observed in lymphocytes of patients following a CT scan may be the result of repair given foci half-life and the time lapse between collection and processing, or due to the detection limit of the assay developed in the lab. However studies such as those by Löbrich have reported the ability to measure  $\gamma$ -H2AX at low and very low doses of ionizing radiation. It could also be the case that low-dose radiation from the CT scan may not be sufficient to activate repair processes and instead may result in cell death or chromosome aberrations, which were both slightly elevated in some patients post CT. Future studies looking at  $\gamma$ -H2AX following *in vivo* exposures to radiation from CT scans should focus the kinetics of foci formation and loss in lymphocytes collected and isolated immediately before and after exposure at a nearby laboratory to fully assess DSB induction

and repair.  $\gamma$ -H2AX has already been described as a potential bioindicator for radiation sensitivity of both normal and malignant tissue. However in this context it is the rate of repair that is of greater importance, although repair fidelity is still in question. That being said, it would also be interesting to look at patient variation in lymphocyte repair kinetics following either a CT scan or a dose as large as 8 Gy.

### ***Adaptive Response***

The adaptive response is a radiobiological phenomenon in which the deleterious effects of a large dose of radiation is reduced following a previous exposure to a smaller ‘priming’ dose of radiation, which is speculated to trigger the activation of repair and antioxidant pathways [43]. Olivieri and Wolff [46] were the first to show that chromosome aberrations were less prominent in lymphocytes exposed to chronic low doses of x-rays prior to a higher challenge dose in comparison to cells treated with a high dose only. The reproducibility of this study and subsequent others which looked at different biological endpoints [15] formed the premise of this part of the Masters Project. It was hypothesized that the *in vivo* dose from the CT scan would be sufficient to upregulate protective mechanisms in the lymphocytes, allowing them to adapt in response to the 3 or 8 Gy *in vitro* challenge doses of Cs<sup>137</sup>  $\gamma$  rays.

A study by Cregan *et al* [47] compared the ability of ionizing radiation versus membrane oxidizing agents in the induction of apoptotic adaptive response. A low dose rate of 0.01 Gy/min  $\gamma$ -rays was delivered to cells as the adaptive treatment, and this was sufficient to significantly increase the level of apoptosis in 8 out of the 12 patients. They

concluded that pre-exposure of lymphocytes to ionizing radiation produced a sensitization to apoptosis which was apparent at 2 Gy and this response is an adaptive mechanism by which cells can eliminate genetic damage. However they also argued the heightened apoptotic effects can confer radiosensitivity for deterministic effects such as skin damage.

The reverse effect was seen in the results of this study, which showed a significant decrease in apoptosis in 3 of the 8 patients, as well as a slight decrease in one patient and an average decrease of ~2 which on a clinical scale is not a concern. The largest decrease in apoptosis was 10%, whereas in the study by Cregan the measured increase in lymphocyte apoptosis was ~26%, however dose conditions were different. Although no distinct pattern was seen for all patients overall, it is still interesting to compare the level of spontaneous apoptosis and apoptosis following a low-dose CT scan with the adaptive response results. For example, patient 5 demonstrated the largest decline in apoptosis following CT, as well in the adaptive experiment (CT + 8 Gy). This patient may be considered radiosensitive based on the reduced radiation-induced apoptotic responses but to fully test this speculation the experiments should be reproduced at a later time.

Another variable that can affect the degree of radioadaptation is the time between the adaptive and challenge doses. Early reviews suggest that a 4-6 hour time period between exposures is required for full activation of pathways and protein synthesis to take place [44]. This is supported by Cregan's work on adaptation kinetics which



displayed a significant increase in radiation-induced apoptosis when the priming dose was given 6 h prior to the challenge dose in comparison to 0 h. Other studies looking at the adaptive response in lymphocytes stimulated into proliferation for endpoints such as mutations administered the priming dose and challenge dose at 24 h and 48 h into culture respectively and still observed a protective effect. For dicentric, the average time difference between the CT scan and the 3 Gy *in vitro* challenge dose was ~3.5 h and interestingly, 5/8 patients displayed a reduction in the frequency of dicentric following CT + Gy in comparison to 3 Gy alone which may suggest an adaptive response. The average difference in frequency, however, was not significant as some patients stayed the same or increased slightly but perhaps these results would have been different if more time was added in between exposures.

The adaptive response is found to be dependent upon factors such as the priming dose, dose rate, irradiation conditions, as well as the cell cycle stage [44, 47]. Although there is strong evidence that adaptation occurs *in vitro*, the concept bears less significance in radioprotection guidelines and risk models that associate IR with carcinogenesis. Some animal studies have observed some level of radioprotection from low doses, including one by Bhattacharjee [56], who pre-irradiated mice with 1 cGy  $\gamma$ -rays for 5 days and noticed a dramatic decrease in the incidence of thymic lymphomas following a challenge dose of 2 Gy in comparison to mice who were irradiated with 2 Gy only. In our lab we continue to perform similar experiments that focus on cancer latency in mice that are cancer prone due to a truncated p53 protein.

## 5. CONCLUSION

The primary goals of this work were to evaluate the degree of inter-individual variation in patients, examine the biological effects of a low dose CT scan, and determine whether this dose was sufficient to induce an adaptive response. Previous experiments in the lab observed the same endpoints in prostate cancer patients in order to develop a predictive assay for radiosensitivity. The results of this study supported two main conclusions: that there is considerable variation in radiation responses, which may have critical implications in determining sensitivity to radiotherapy, and that lymphocytes responds to low and high doses of radiation differently. This work also corroborates mounting evidence which suggests that the LNT model may not be ideal in predicting risk at low dose exposures. Due to the high degree of variation amongst patients, spontaneous levels of apoptosis were not able to determine how the cells will respond to CT radiation or a large *in vitro* dose of gamma rays. Similarly, there was no apparent correlation between the induction of apoptosis after CT and that observed after 8 Gy. While some patients exhibited an increase in apoptosis following both exposures, others showed reversed responses or no changes at all. The CT scan also showed no significant biological effect in the formation of  $\gamma$ -H2AX foci and dicentric, however a dramatic increase in both endpoints was observed following a larger dose which was expected due to the induction of DNA DSBs. The adaptive response was observed for all endpoints but not all patients, which again exemplifies the variation in sensitivity.

These results spur debate regarding the detection limit for each endpoint and corresponding assay performed. While many studies have shown that at low (<100 mGy) and very low (1-10mGy) doses biological effects can be measured, perhaps additional dose and kinetic studies with lymphocytes should be performed to optimize the signal and determine the appropriate time point to measure changes. The adaptive response, in particular, is a process by which a cell must first upregulate genes involved in repair and antioxidant pathways in order for it to establish inherent radioprotection.

Additional methods which measure these endpoints can help determine with better accuracy the mechanisms taking place during and after irradiation treatment. For example, flow-based assays that measure other steps in the apoptotic pathway such alterations in mitochondrial transmembrane potential, measured through DiOC<sub>6</sub> activity, and caspase activation can confirm with more certainty that cells are undergoing radiation-induced programmed cell death. It has also been shown that alternative routes may be taken by a cell to repair and eliminate genetic damage, which require many key proteins as well as cross-talk between different signal transduction pathways. Mutation experiments may establish which proteins are most important during specific cellular responses, for example altering the H2AX histone in order to determine if a cell can still undergo repair in the absence of phosphorylation.

Finally, gene expression analysis experiments may also prove valuable for this study. Molecular methods observing p53 or ATM activation can shed more light on the mechanisms that give rise to variation in radiation responses. Overall, although this

research shows that low dose radiation from a CT scan does not significantly affect levels of lymphocyte death and DNA damage, there still exists a concern for health risks that imaging modalities pose patients whom require their use. To eliminate any exposure to ionizing radiation, physicians may also use magnetic resonance imaging to observe and contour internal structures. However in comparison to CT, MRI provides less detail on bone anatomy, is much more costly and often associated with greater discomfort for the patient.

## 6. REFERENCES

1. Department of Energy Report YMP-0337 from BEIR IV, from <http://www.ocrwm.doe.gov/factsheets/pdf/ymp0337rev1.pdf>
2. World Health Organization, Department of Essential Health Technologies. *Essential Diagnostic Imagine*, [online] accessed December 14, 2010, from < <http://www.who.int/eht/en/DiagnosticImaging.pdf>>
3. Canadian Institute for Health Information. *Medical Imaging in Canada 2007*, [online] accessed December 1, 2010, from < [http://secure.cihi.ca/cihiweb/products/MIT\\_2007\\_e.pdf](http://secure.cihi.ca/cihiweb/products/MIT_2007_e.pdf)>
4. Lee Z, Sodee DB, Resnick M, MacLennan GT. Multimodal and three-dimensional imaging of prostate cancer. *Computerized Med Imaging and Graphics* 2005; 29: 477-486
5. Chodick G, Ronckers CM, Shalev V, Ron E. Excess Lifetime Cancer Mortality Risk Attributable to Radiation Exposure from Computed Tomography Examinations in Children. *IMAJ* 2007; 9: 584-587
6. International Commission on Radiological Protection (ICRP). *Managing Patient Dose in Multi-Detector Computed Tomography (MDCT)*, 2006 [online] accessed November 2010, from < [http://www.icrp.org/docs/ICRP-MDCT-for\\_web\\_cons\\_32\\_219\\_06.pdf](http://www.icrp.org/docs/ICRP-MDCT-for_web_cons_32_219_06.pdf)>
7. Brenner DJ. Estimating cancer risks from pediatric CT: Going from the qualitative to the quantitative. *Pediatric Radiology* 2002; 32: 228-231
8. Stephan G, Schneider K, Panzer W, Walsh L, Oestreicher U. Enhanced yield of chromosome aberrations after CT examinations in paediatric patients. *Int J Radiat Biol.* 2007; 83(5): 281-287
9. Ward JF. The complexity of DNA Damage: relevance to biological consequences. *Int J Radiat Bio* 1994; 66(5): 427-432

10. Ward JF. DNA Damage Produced by Ionizing Radiation in Mammalian Cells: Identities, Mechanisms of Formation, and Reparability. *Progress in Nucleic Acid Research and Molecular Biology* 1988; 95-125
11. Jeggo P, Lavin MF. Cellular radiosensitivity: How much better do we understand it? *Int J Radiat Biol* 2009; 85(12): 1061-1081
12. Hall EJ. Radiobiology for the Radiologist, 6<sup>th</sup> ed. Philadelphia, PA: Lippincott Williams & Wilkins, 2006
13. Verheij M, Bartelink H. Radiation-induced apoptosis. *Cell Tissue Res* 2000; 301: 133-142
14. Rigaud O, Moustacchi E. Radioadaptation for gene mutation and the possible molecular mechanisms of the adaptive response. *Mut Research* 1996; 358: 127-134
15. Tapio S, Jacob V. Radioadaptive response revisited. *Radiat Environ Biophysics* 2007; 46: 1-12
16. Anderson RE, Warner NL. Ionizing radiation and the immune response. *Adv Immunol* 1976; 24: 215-335
17. Payne CM, Bjore CG, Schultz DA. Change in the frequency of apoptosis after low-and high-dose X-irradiation of human lymphocytes. *J Leuk Biol.* 1992; 52: 433-439
18. International Atomic Energy Agency. *Cytogenetic Analysis for Radiation Dose Assessment: A Manual*, Technical Reports Series No. 405. Vienna, 2001 [online] accessed November 10, 2010, from <  
[http://wwwpub.iaea.org/MTCD/publications/PDF/TRS405\\_scr.pdf](http://wwwpub.iaea.org/MTCD/publications/PDF/TRS405_scr.pdf)>
19. Nowell PC. Phytohemagglutinin: an initiator of mitosis in cultures of normal human leukocytes. *Cancer Res* 1960; 20: 462.



20. Andrievski A, Wilkins RC. The response of  $\gamma$ -H2AX in human lymphocytes and lymphocyte subsets measured in whole blood cultures. *Int J Radiat Biol.* 2009; 85(4): 369-376
21. Schnarr K, Boreham D, Sathya J, Julian J, Dayes IS. Radiation-Induced Lymphocyte Apoptosis to Predict Radiation Therapy Late Toxicity in Prostate Cancer Patients. *Int J Radiat Biol. Phys.* 2009; 74(5): 1424-1430
22. Majno G, Joris I. Apoptosis, Oncosis, and Necrosis: An Overview of Cell Death. *American Journal of Pathology* 1995; 146: 3-15
23. Wilkins RC, Wilkinson D, Maharaj HP, Bellier PV, Cybulski MB, McLean JRN. Differential apoptotic responses to ionizing radiation in subpopulations of human white blood cells. *Mut Research* 2002; 513: 27-36
24. Hertveldt K, Philippe J, Thierens H, Cornelissen M, Vral A, De Ridder L. Flow cytometry as a quantitative and sensitive method to evaluate low dose radiation induced apoptosis *in vitro* in human peripheral blood lymphocytes. *Int Journal Rad Bio* 1997; 4: 429-433
25. Shinomiya N. New concepts in radiation-induced apoptosis: 'premitotic apoptosis' and 'postmitotic apoptosis'. *J of Cellular and Mol Med* 2001; 5(3): 240-253
26. Kerr JFR, Wyllie AH, Currie AR. Apoptosis: a basic biological phenomenon with wide-ranging implications in tissue kinetics. *Br J Cancer* 1972; 26: 239-257
27. Cregan SP, Smith BP, Brown DL, Mitchel REJ. Two pathways for the induction of apoptosis in human lymphocytes. *Int J Rad Biol* 1999; 75(9): 1069-1086
28. Vijayalaxmi, Burkart W. Resistance and cross-resistance to chromosome damage in human blood lymphocytes to bleomycin. *Mut Res.* 1989; 211: 45-50
29. Boreham DR, Gale K, Maves S, Walker JA, Morrison DP. Radiation-induced apoptosis in human lymphocytes: Potential as a biological dosimeter. *Health Physics* 1996; 71(5): 685- 691

30. Schnarr K, Dayes I, Sathya J, Boreham D. Individual Radiosensitivity and its Relevance to Health Physics. *Dose-Response* 2007; 5: 333-348
31. Ito Y, Otsuki Y. Localization of Apoptotic Cells in the Human Epidermis by an In Situ DNA Nick End-labeling Method using Confocal Reflectant Laser Microscopy. *J Histochem Cytochem* 1998; 46: 783-786
32. Ozgen U, Savasan S, Buck S, Ravindranath Y. Comparison of DiOC<sub>6</sub>(3) Uptake and Annexin V Labeling for Quantification of Apoptosis in Leukemia Cells and Non-Malignant T Lymphocytes From Children. *Cytometry* 2000; 42: 74-78.
33. Vermes I, Haanen C, Steffans-Nakken H, Reutelingsperger C. A Novel assay for apoptosis Flow cytometric detection of phosphatidylserine expression on early apoptotic cells: using Fluorescein labeled Annexin V. *Journal of Immun Methods* 1995; 184: 39-51
34. Bonner WM, Redon CE, Dickey JS, Nakamura AJ, Sedelnikova OA, Solier S, Pommier Y.  $\gamma$ H2AX and Cancer. *Nature Reviews Cancer* 2008; 8: 957-967
35. Huang X, Darzynkiewicz Z. Cytometric Assessment of Histone H2AX Phosphorylation. *Methods Mol Biol* 2006; 314: 73-80
36. Rogakou EP, Boon C, Redon C, Bonner WM. Megabase Chromatin Domains Involved in DNA Double-Strand Breaks In Vivo. *Journal of Cell Biol.* 1999; 146: 905-915
37. Löbrich M, Rief N, Kuhne M, Heckmann M, Fleckenstein J, Rube C. *In vivo* formation and repair of DNA double-strand breaks after computed tomography examinations *Proc Natl Acad Sci* 2005; 102(25): 8984-8989
38. Pinto MMP, Santos NFG, Amaral A. Current status of biodosimetry based on standard cytogenetic methods. *Radiat Environ Biophysics* 2010; 49: 567-581
39. Prasanna PGS, Moroni M, Pellmar TC. Triage Dose Assessment for Partial-Body Exposure: Dicentric Analysis *Health Physics* 2010; 98(2): 244-251

40. International Standardization Organization. Radiation protection performance criteria for service laboratories performing biological dosimetry by cytogenetics. Geneva: ISO Office; ISO19238; 2004
41. Cramers P, Atanasova P, Vrolijk H, Darroudi F, van Zeeland AA, Huiskamp R, Mullenders LHF, Kleinjans JCS. Pre-exposure to Low Doses: Modulation of X-ray-Induced DNA Damage and Repair? *Rad Res* 2005; 164: 383-390
42. Shadley JD. Chromosomal Adaptive Response in Human Lymphocytes. *Rad Res* 1994; 138: S9-S12
43. Rigaud O, Moustacchi E. Radioadaptation for gene mutation and the possible molecular mechanisms of the adaptive response. *Mut Res* 1996; 358: 127-134
44. Wolff S. The adaptive response in radiobiology: evolving insights and implications. *Environ Health Perspect* 1998; 106: 277-283
45. Ikushima T. Chromosomal responses to ionizing radiation reminiscent of an adaptive response in cultured Chinese hamster cells. *Mut Res* 1987; 180: 215-221
46. Olivieri G, Bodycote Y, Wolff S. Adaptive response of human lymphocytes to low concentrations of radioactive thymidine. *Science* 1984; 223: 594-597
47. Cregan SP, Brown DL, Mitchel REJ. Apoptosis and the adaptive response in human lymphocytes. *Int J Rad Biol* 1999; 75: 1087-1094
48. Cortes F, Dominguez J, Pinero J, Mateos JC. Adaptive response in human lymphocytes conditioned with hydrogen peroxide before irradiation with x-rays. *Mutagenesis* 1990; 5: 555-557.
49. Vral A, Cornelissen M, Thierens H, Louagie H, Philippe J, Strijckmans K, De Ridder L. Apoptosis induced by fast neutrons versus  $^{60}\text{Co}$   $\gamma$ -rays in human peripheral blood lymphocytes. *Int J Rad Biol* 1998; 73(3): 289-295
50. Thierens H, Vral A, Barbe M, Meijlaers M, Baeyens A, De Ridder L. Chromosome radiosensitivity study of temporary nuclear workers and the support

- of the adaptive response induced by occupational exposure. *Int J Radiat Biol* 2002; 78(12): 1117-1126
51. Ghiassi-nejad M, Mortazavi SMJ, Cameron JR, Niroomand-rad A, Karam PA. Very High Background Radiation Areas of Ramsar Iran: Preliminary Biological Studies. *Health Physics* 2002; 82(1): 87-89
52. Leong T, Borg M, McKay M. Clinical and Cellular Radiosensitivity in Inherited Human Syndromes. *Clinical Oncology* 2004; 16: 206-209
53. Floyd DN, Cassoni AM. Intrinsic radiosensitivity of adult and cord blood lymphocytes as determined by the micronucleus assay. *Eur J Cancer* 1994; 5: 615-620
54. Fei P, El-Deiry WS. P53 and radiation responses. *Oncogene* 2003; 22: 5774-5783
55. Tubiana M, Aurengo A, Averbeck D, Masse R. Recent reports on the effect of low doses of ionizing radiation and its dose-effect relationship. *Radiat Environ Biophysics* 2006; 44: 245-251
56. Bhattacharjee D. Role of radio-adaptation on radiation-induced thymic lymphoma in mice. *Mut Res* 1996; 358: 231-235
57. Carbonari M, Cibati M, Cherchi M, Sbarigia D, Pesce AM, Dell'Anne L, Modica M, Fiorilli M. Detection and Characterization of Apoptotic Peripheral Blood Lymphocytes in Human Immunodeficiency Virus Infection and Cancer Chemotherapy by a Novel Flow Immunocytometric Method. *Blood* 1994; 83(5): 1268-1277
58. Gelman R, Wilkening C. Analyses of Quality Assessment Studies Using CD45 for Gating Lymphocytes for CD3<sup>+</sup>4<sup>+</sup>%. *Cytometry* 2000; 42: 1-4
59. Schmitz A, Bayer J, Dechamps N, Thomas G. Intrinsic Susceptibility to Radiation-Induced Apoptosis of Human Lymphocyte Subpopulations. *Int J Radiation Onc* 2003; 3: 769-778

60. Olive PL, Banath JP. Phosphorylation of Histone H2AX as a Measure of Radiosensitivity. . *Int J Radiation Onc* 2004; 2: 331-335
61. Jones LA, Scott D, Cowan R, et al: Abnormal radiosensitivity of lymphocytes from breast cancer patients with excessive normal tissue damage after radiotherapy: Chromosome aberrations after low dose-rate irradiation. *Int J Radiat Biol* 1995; 67: 519-528
62. Barber, JBP, West CML, Kiltie AE, Roberts SA, Scott D. Detection of Individual Differences in Radiation-Induced Apoptosis of Peripheral Blood Lymphocytes in Normal Individuals, Ataxia Telangiectasia Homozygotes and Heterozygotes, and Breast Cancer Patients after Radiotherapy. *Rad Res* 2000; 153(5): 570-578
63. Miller SM, Ferrarotto CL, Vlahovich S, Wilkins RC, Boreham DR, Dolling J. Canadian Cytogenetic Emergency Network (CEN) for biological dosimetry following radiological/nuclear accidents. *Int J Rad Biol* 2007; 83: 471-477
64. M'Kacher R, Violet D, Aubert B, Grinsky T, Dossou J, Béron-Gaillard N, Carde P, Parmentier C. Premature chromosome condensation associated with fluorescence *in situ* hybridization detects cytogenetic abnormalities after a CT scan: Evaluation of the low-dose effect. *Radiat Prot Dos* 2003; 103(1) 35-29
65. Feinendegen LE, Pollycove M, Neumann RD. Low-dose cancer risk modeling must recognize up-regulation of protection. *Dose-Response* 2010; 8: 227-252
66. Académie Nationale de Médecine, Institute de France – Académie des Sciences Joint Report n2 (March 20, 2005) Tubiana M, Aurengo A, Averbeck D, Bonnin A, Le Guen E, Masse R, Monier R, Valleron AJ, de Wathaire F. Dose-effect relationships and the estimation of the carcinogenic effects of low doses of ionizing radiation  
<http://www.radscihealth.org/rsh/Docs/Correspondence/BEIRVII/TubianaAurengo5Oct05.pdf>
67. Collis SJ, Schwaninger JM, Ntambi AJ, Keller TW, Nelson WG, Dillehay LE, DeWeese TL. Evasion of Early Cellular Response Mechanisms following Low Level Radiation-induced DNA Damage. *J Biol Chem* 2004; 279(48): 49624-49632

68. Beels L, Werbrouck J, Thierens H. Dose response and repair kinetics of  $\gamma$ -H2AX foci induced by in vitro irradiation of whole blood and T-lymphocytes with X- and  $\gamma$ -radiation. *Int J Radiat Biol* 2010; 86(9): 760-768
69. Rothkamm K, Löbrich M. Evidence for a lack of DNA double-strand break repair in human cells exposed to very low x-ray doses. *Proc Natl Acad Sci* 2003; 100(9): 5057-5062
70. Krueger SA, Joiner MC, Weinfeld M, Piasentin E, Marples B. Role of Apoptosis in Low-Dose Hyper-radiosensitivity. *Rad Res* 2007; 167: 260-267
71. Joiner MC, Lambin P, Malaise EP, Robson T, Arrand JE, Skov KA, Marples B. Hypersensitivity to very-low single radiation doses: Its relationship to the adaptive response and induced radioresistance. *Mutation Res* 1996; 358: 171-183
72. Williams GT. Programmed Cell Death: Apoptosis and Oncogenesis. *Cell* 1991; 65: 1097-1097
73. Kondo S. Altruistic cell suicide in relation to radiation hormesis. *Intern J Radiat Biol* 1988; 53: 95–102
74. Orrenius S, Zhivotovsky B, Nicotera P. Regulation of cell death: the calcium-apoptosis link. *Nature Reviews Mol Cell Biol* 2003; 4: 552-565
75. Abraham RT. Checkpoint signaling: focusing on 53BP1. *Nature Cell Biology* 2002; 4: E277-E279
76. National Council on Radiation Protection & Measurements *Report No. 116 - Ionizing Radiation Exposure of the Population of the United States*

# **APPENDIX**



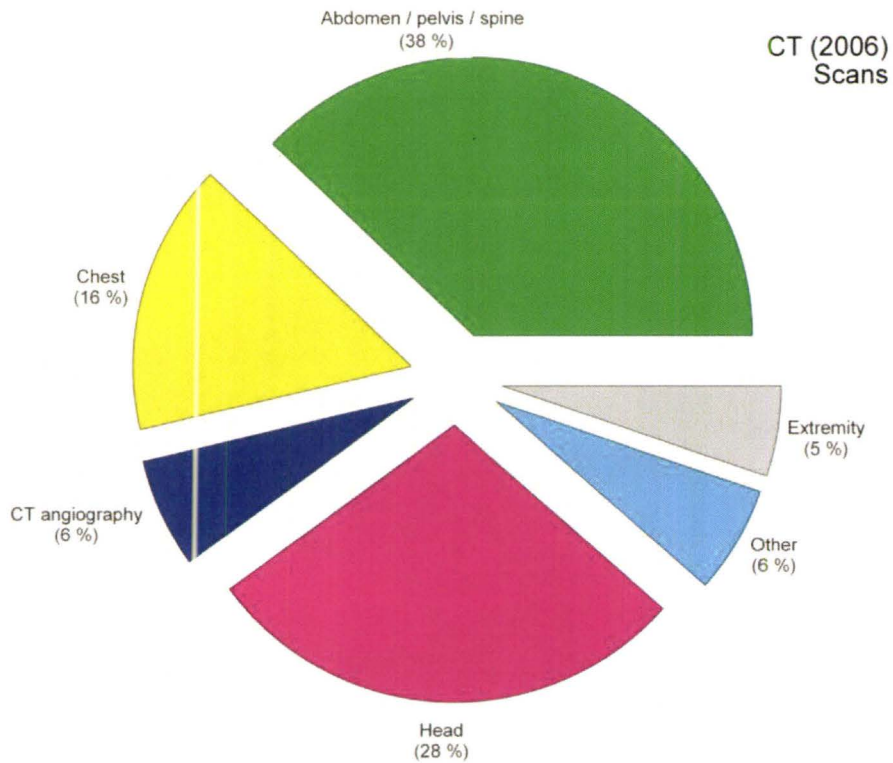


**Figure A-1: Percent contribution of CT scan types to total number of scans (67 million) in 2006\***

**\*Source: NCRP Report No. 160 Section 4**

**<[http://www.ncrponline.org/images/160\\_pie\\_charts/Fig4-2.pdf](http://www.ncrponline.org/images/160_pie_charts/Fig4-2.pdf)>**

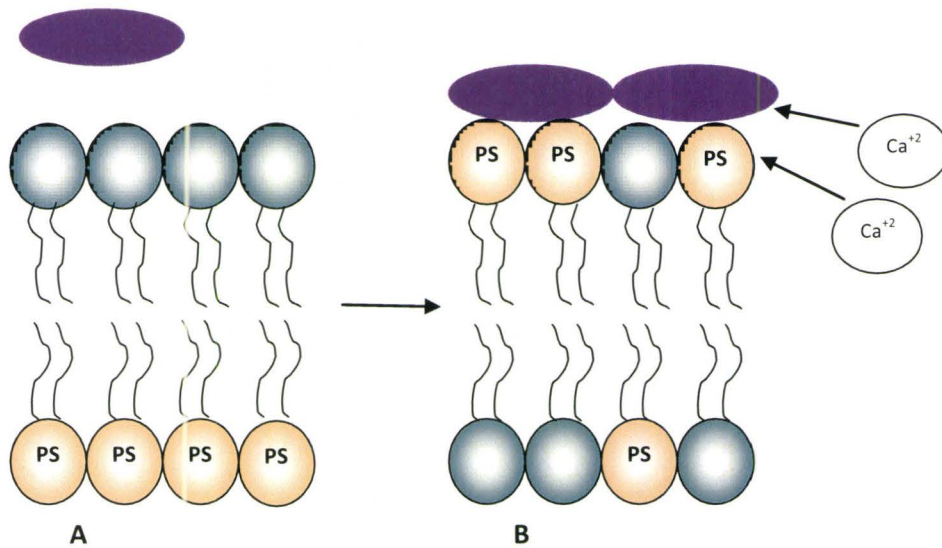


**Figure A-2: In normal cells (A) there is an asymmetry in the cell membrane and phosphatidylserine is typically located on the inner leaflet (bottom layer). In apoptotic cells (B) PS is externalized on the outer leaflet (top) of the membrane and can be detected by Annexin V (Purple)\***

\*Adapted from Orrenius et al. *Nature Reviews Molecular Cell Biology* 2003; 4<sup>74</sup>

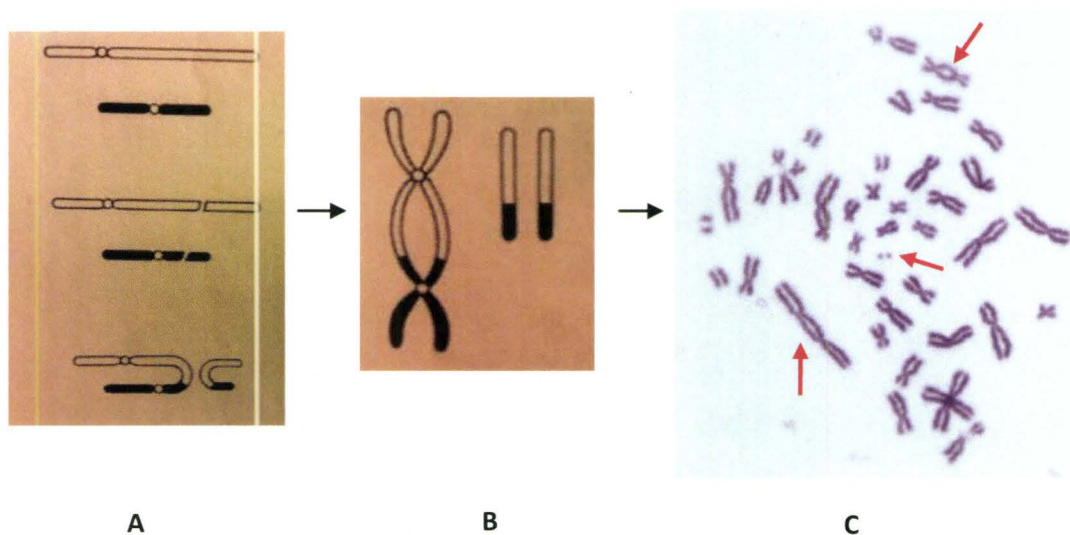


**Figure A-3: Steps in the formation of a dicentric chromosome.** The interaction of the cell nucleus with energy from ionizing radiation can produce genomic lesions. If breaks occur in two separate pre-replication or  $G_1$  chromosomes (A), they as well as their corresponding broken DNA fragments can join. When replication occurs in the S phase (B), there now exists two sister chromatids that also join at the sticky ends, forming a grossly distorted chromosome with two centromeres. Under a microscope (C) the dicentrics and their acentric fragments (chromosomes with no centromeres), indicated by the red arrows, are scored within each metaphase. The first two images are taken from Hall 6<sup>th</sup> edition *Radiobiology for the Radiologist* 2006<sup>12</sup>

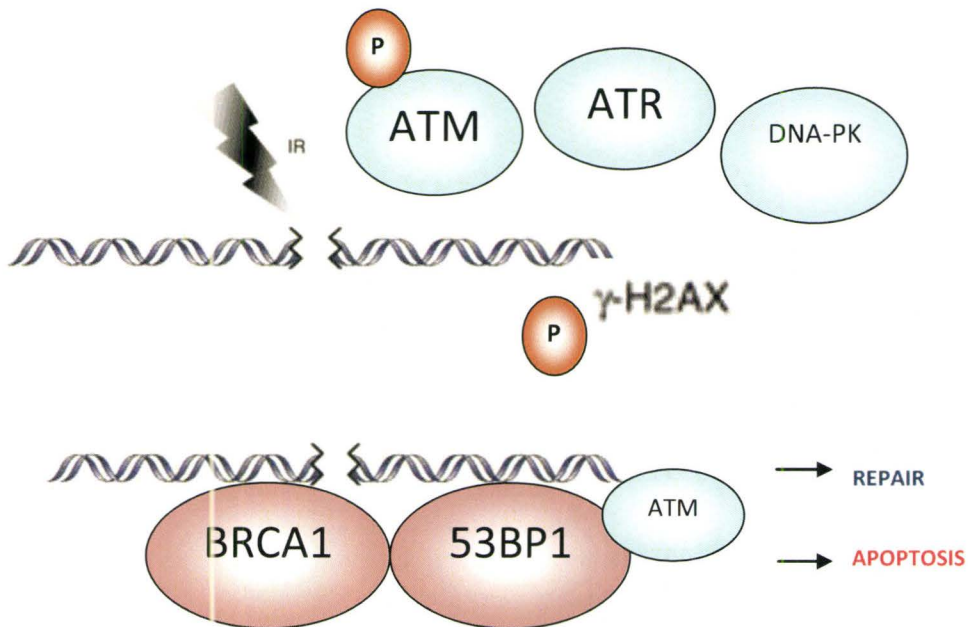
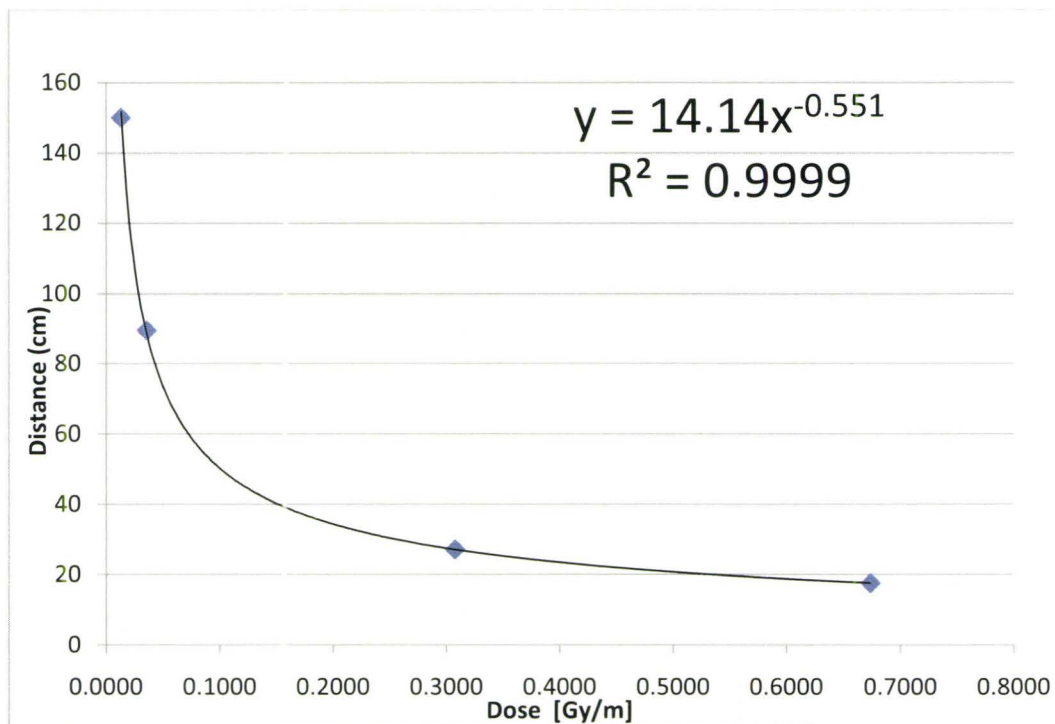


**Figure A-4: DNA strand breaks produced by ionizing radiation and other genotoxic agents can be immediately detected by members of the Phosphatidylinositol 3-kinase-related kinase (PIKK) family (ATM, ATR and DNA-PK) as well as other sensor proteins. ATM in particular undergoes autophosphorylation (P) and subsequently phosphorylates the histone protein H2AX at amino acid Ser-139. Formation of  $\gamma$ -H2AX by this phosphorylation event is required for the recruitment of DNA repair factors such as 53BP1 and BRCA1. 53BP1 also functions to couple ATM with additional downstream targets including p53. The primary outcome of this pathway is damage repair, however the cell can also undergo apoptosis following  $\gamma$ -H2AX induction\***

\*Adapted from Abraham *Nature Cell Biology* 2002; 4<sup>75</sup>

**Cesium-137 Source: Dose Rate (mGy min<sup>-1</sup>) vs Distance (cm) April 20, 2010**



Distance calculation for dose rate: 0.1 Gy/min

y = Distance

x=Dose rate

Relationship:

$$y = 14.14x^{-0.551}$$

$$= 14.14(0.1)^{-0.551}$$

$$= 50.29\text{cm} - 6\text{cm (distance from source to opening)}$$

$$= 44.29 \text{ cm from opening to surface*}$$

\*surface refers to bottom of flat side tube for DCA and bottom of T25 flask for apoptosis/H2AX

**Figure B-1: Dose rate map for the Taylor Radiobiology Facility Cs<sup>137</sup> gamma ray source at McMaster University. Updated April 2010**



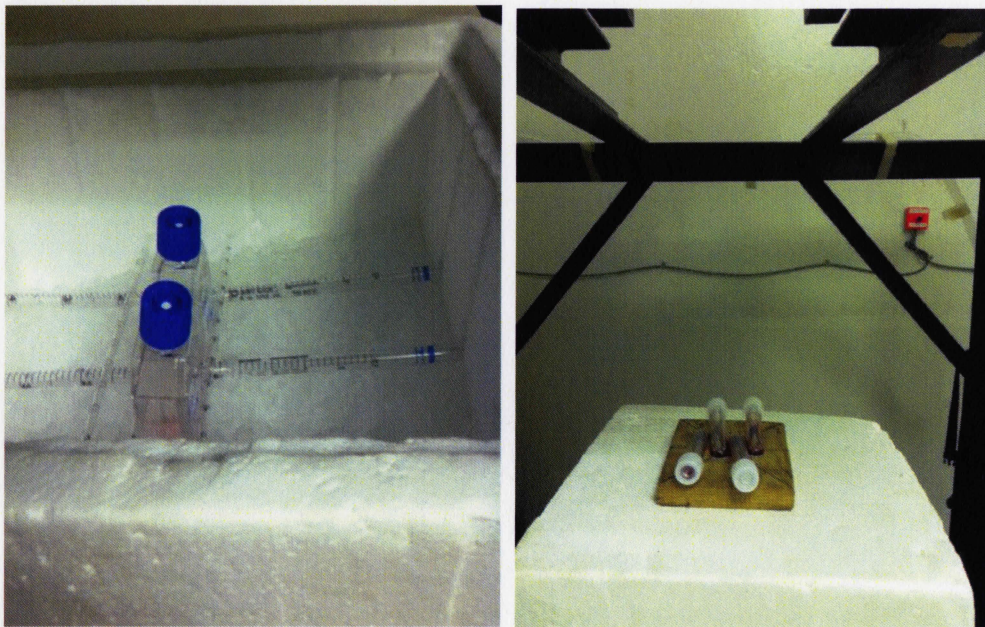


**Figure B-2: Irradiation set-up at the Taylor source. For apoptosis and  $\gamma$ -H2AX, isolated lymphocytes in supplemented media were aliquoted into duplicate T25 flasks (Left) and irradiated on ice 44.29 cm (dose rate = 0.1 Gy/min) from the opening of the  $\text{Cs}^{137}$  source. For the dicentric assay, 0.5 ml of whole blood was irradiated in flat-side tubes (Right) at room temperature 44.29 cm from the opening of the source**

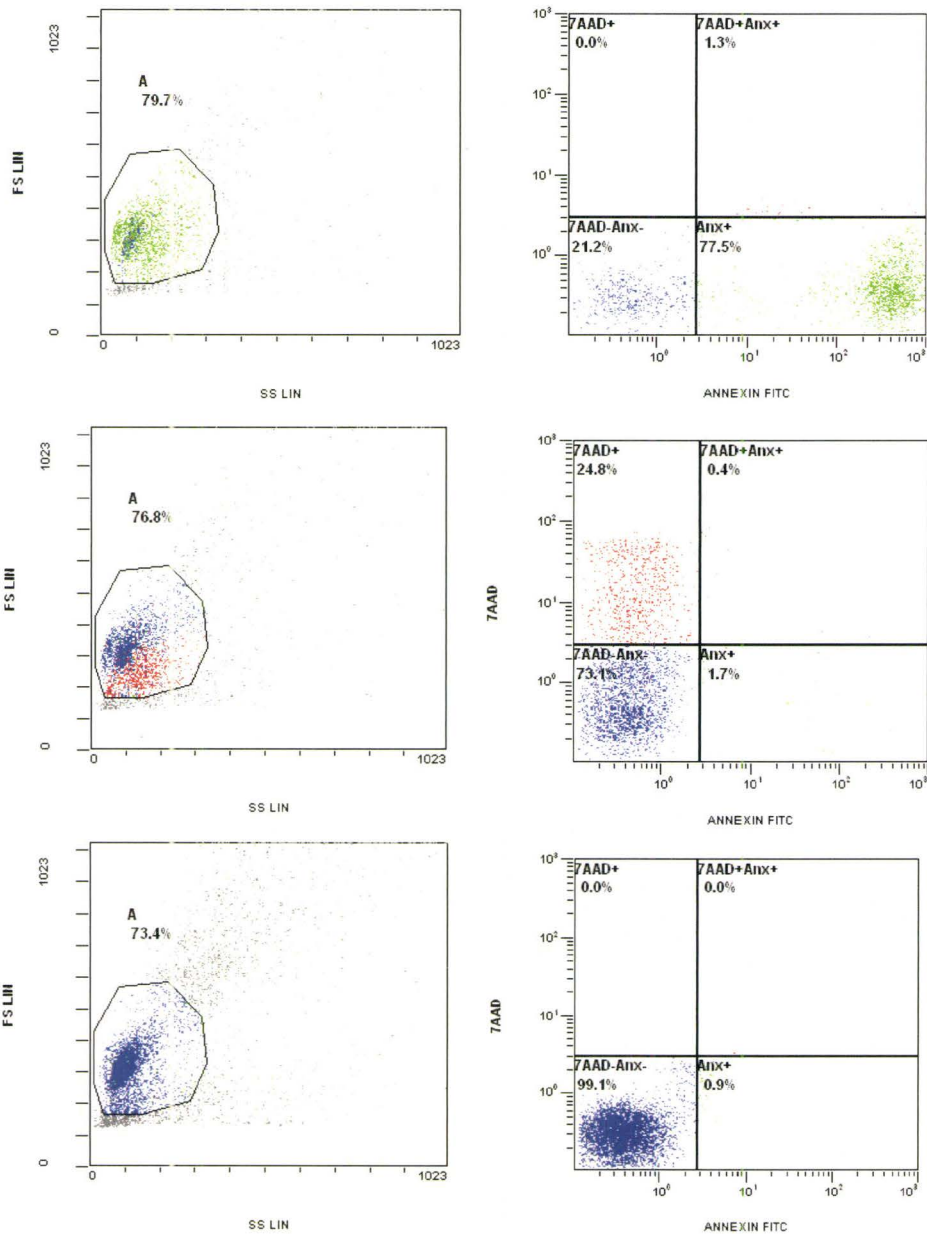


**Figure B-3: Dot plots of controls from Annexin-FITC/7AAD apoptosis assay. Isolated lymphocytes were adjusted to  $5 \times 10^5$  cells/ml and labeled with either Annexin only (A), 7AAD only (B) and an unstained control (C) prior to flow analysis. Annexin was analyzed for green fluorescence (FITC – green dots) and red fluorescence (7AAD – red dots). Blue dots indicate those cells that are negative for both Annexin and 7AAD (bottom left quadrant). L Panel: Lymphocytes gates on forward scatter (FS) and side scatter (SS) patterns. R Panel: Percentage of Gate A that is positive for Annexin**



<b>CT</b>			
<b>PATIENT</b>	<b>PRE CT (%) - SPONTANEOUS</b>	<b>POST CT (%)</b>	<b>DIFFERENCE</b>
1	39.00	46.77	7.77
2	24.90	26.54	1.64
3	32.78	36.39	3.60
4	17.66	16.48	-1.18
5	50.62	38.11	-12.51
6	34.67	34.91	0.24
7	40.68	38.61	-2.07
8	26.14	27.39	1.25
<b>Average</b>	<b>33.31</b>	<b>33.15</b>	<b>-0.16</b>

A

<b>8 Gy CHALLENGE</b>			
<b>PATIENT</b>	<b>0 GY (%)</b>	<b>8 GY (%)</b>	<b>DIFFERENCE</b>
1	39.00	75.06	36.06
2	24.90	81.47	56.57
3	32.78	81.18	48.40
4	17.66	64.73	47.07
5	50.62	86.99	36.37
6	34.67	76.17	41.50
7	40.68	68.73	28.05
8	26.14	74.56	48.42
<b>Average</b>	<b>33.31</b>	<b>76.11</b>	<b>42.81</b>

B

<b>ADAPTIVE</b>			
<b>PATIENT</b>	<b>PRE CT + 8 GY (%)</b>	<b>POST CT + 8 GY (%)</b>	<b>DIFFERENCE</b>
1	75.06	76.02	0.96
2	81.47	82.62	1.15
3	81.18	77.44	-3.74
4	64.73	67.17	2.44
5	86.99	77.39	-9.6
6	76.17	74.54	-1.63
7	68.73	66.38	-2.35
8	74.56	74.98	0.42
<b>Average</b>	<b>76.11</b>	<b>74.57</b>	<b>-1.54</b>

C

**Table C-1: Comparison data for all patients. These tables show the percept difference following different radiation treatments. A) Difference before and after CT B) Difference before and after 8 Gy *in vitro* C) Difference between 8 Gy only (left) and 8 Gy following CT scan (right). For all tables, negative values indicate a decrease before and after CT**

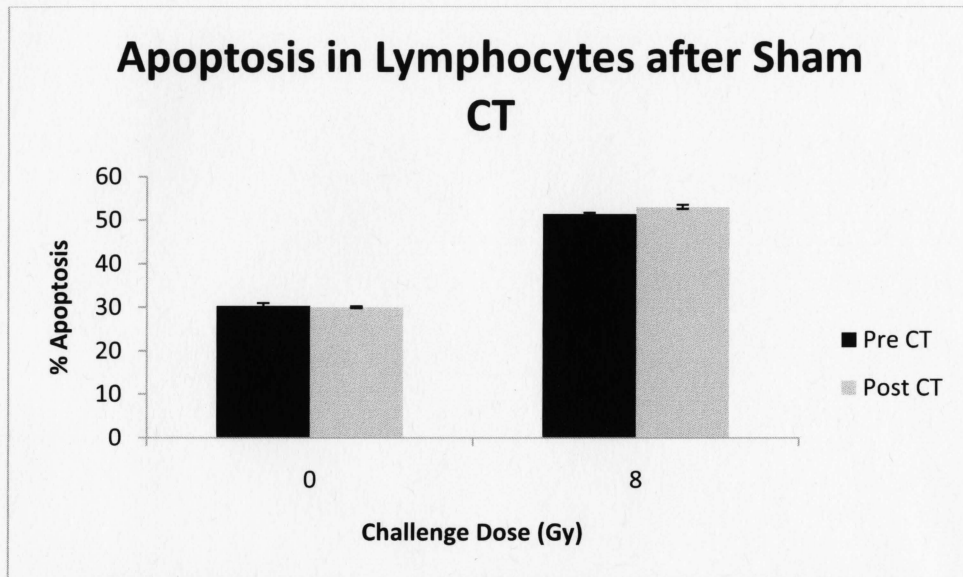


**Figure C-1: Percent apoptosis results from sham CT control experiment. Lymphocytes that were collected before and after sham CT were also irradiated *in vitro* with 8 Gy apoptosis was compared before and after treatment**